

SYNTHESIS OF PROPORTIONAL-INTEGRAL-DERIVATIVE CONTROLLER  
FROM EMPIRICAL DATA AND GUARANTEEING PERFORMANCE  
SPECIFICATIONS

A Thesis  
by  
DONGWON LIM

Submitted to the Office of Graduate Studies of  
Texas A&M University  
in partial fulfillment of the requirements for the degree of

MASTER OF SCIENCE

May 2008

Major Subject : Mechanical Engineering

SYNTHESIS OF PROPORTIONAL-INTEGRAL-DERIVATIVE CONTROLLER  
FROM EMPIRICAL DATA AND GUARANTEEING PERFORMANCE  
SPECIFICATIONS

A Thesis  
by  
DONGWON LIM

Submitted to the Office of Graduate Studies of  
Texas A&M University  
in partial fulfillment of the requirements for the degree of

MASTER OF SCIENCE

Approved by :

Chair of Committee,	Darbha Swaroop
Committee Members,	Bryan Rasmussen
	Shankar P. Bhattacharyya
Head of Department,	Dennis O'Neal

May 2008

Major Subject : Mechanical Engineering

## ABSTRACT

Synthesis of Proportional-Integral-Derivative Controller from Empirical Data and

Guaranteeing Performance Specifications. (May 2008)

Dongwon Lim, B.S., Hanyang University, Seoul, Korea

Chair of Advisory Committee: Dr. Darbha Swaroop

For a long time determining the stability issue of characteristic polynomials has played a very important role in Control System Engineering. This thesis addresses the traditional control issues such as stabilizing a system with any certain controller analyzing characteristic polynomial, yet a new perspective to solve them. Particularly, in this thesis, Proportional-Integral-Derivative (PID) controller is considered for a fixed structured controller. This research aims to attain controller gain set satisfying given performance specifications, not from the exact mathematical model, but from the empirical data of the system. Therefore, instead of a characteristic polynomial equation, a specially formulated characteristic rational function is investigated for the stability of the system in order to use only the frequency data of the plant. Because the performance satisfaction is highly focused on, the characteristic rational function for the investigation of the stability is mainly dealt with the complex coefficient polynomial case rather than real one through whole chapters, and the mathematical basis for the complex case is prepared.

For the performance specifications, phase margin is considered first since it is a very significant factor to examine the system's nominal stability extent (nominal

performance). Second, satisfying  $H_\infty$  norm constraints is handled to make a more robust closed loop feedback control system. Third, we assume undefined, but bounded outside noise, exists when estimating the system's frequency data. While considering these uncertainties, a robust control system which meets a given phase margin performance, is attained finally (robust performance).

In this thesis, the way is explained how the entire PID controller gain sets satisfying the given performances mentioned in the above are obtained. The approach fully makes use of the calculating software e.g. MATLAB<sup>®</sup> in this research and is developed in a systematically and automatically computational aspect. The result of synthesizing PID controller is visualized through the graphic user interface of a computer.

To my beloved newborn son – my treasure

## ACKNOWLEDGMENTS

Most of all, I would like to thank my academic advisor Dr. Darbha Swaroop for his noble suggestions, consideration, and encouragement to finish my work, but above all, for his ceaseless support. Because of him, I encountered the latest research in the field of control systems. He made me realize that my interest and qualifications are well suited to this research area. With his guidance, pushing and correcting, he made me realize I could make it within the planned time. I would like to thank Dr. Bhattacharyya for allowing me to sit in his “Linear Control Theory” class. I was able to be exposed to systematic broad knowledge related to my research, and I became aware of more existing papers from other experienced people. I would also like to thank Dr. Rasmussen for his time and thoughtfulness. His co-operation played a great part in the successful completion of this work.

In addition, I would like to thank Dr. Waqar Malik for his advice and interest in my research. He was the author of the dissertation which I first referred to in my research. He shared his time and gave me very sincere advising.

Last, but never the least, I would like to thank my wife, Chahee Lee, for her endless spiritual and physical support. Without her, I couldn't imagine finishing this work.

## TABLE OF CONTENTS

CHAPTER	Page
I	INTRODUCTION ..... 1
	A. Objective ..... 3
	B. Organization of Thesis ..... 4
II	MATHEMATICAL PRELIMINARIES ..... 5
	A. Introduction ..... 5
	B. Mikhailov's Criterion ..... 6
	C. Hermite-Biehler Theorem for Complex Polynomials ..... 9
	D. Generalization of the Hermite-Biehler Theorem ..... 10
	E. Algorithm for Automatic Sign Assignment ..... 17
III	FIXED STRUCTURE CONTROLLER SYNTHESIS FOR PHASE MARGIN PROPERTY ..... 22
	A. Introduction ..... 22
	B. Theory and Algorithm ..... 23
	C. Determination of Controller Parameter Set ..... 27
	D. Illustrative Examples ..... 31
IV	FIXED STRUCTURE CONTROLLER SYNTHESIS FOR $H_\infty$ NORM CONSTRAINT ..... 44
	A. Introduction ..... 44
	B. Background Theory ..... 45
	C. Expansion of Characteristic Equation for PID Controllers and Algorithm ..... 46
	D. Illustrative Examples ..... 50
V	ROBUST PID CONTROLLER SYNTHESIS FROM EMPIRICAL DATA ..... 61
	A. Introduction ..... 61
	B. Determining Robust PID Controller Set ..... 62

CHAPTER	Page
C. Examples .....	67
VI CONCLUSION AND FUTURE WORK .....	76
A. Summary .....	76
B. Future Work .....	77
REFERENCES .....	78
VITA .....	81



## LIST OF FIGURES

FIGURE	Page
1 Mikhailov's plot for Hurwitz complex polynomial .....	7
2 Mikhailov's plot for Example II.1 .....	8
3 Interlacing property for a Hurwitz polynomial .....	10
4 Mikhailov's plot .....	15
5 Magnified Mikhailo'v plot of Fig.3. ....	15
6 Decomposition into real and imaginary part .....	16
7 Magnification of Fig. 6. ....	16
8 Bode plot of the plant's frequency response .....	32
9 Nyquist plot of the plant's frequency response .....	32
10 Plot of $f(\omega)$ with respect to the frequency .....	34
11 Magnification of Fig. 10 .....	34
12 $\delta_i(\omega)$ plot to examine its real roots .....	35
13 Entire $K_d, K_i$ controller set satisfying $PM > 30^\circ$ .....	36
14 Bode diagram and step response of the system by the selected controller .....	37
15 Entire PID controller set for Example III.1 .....	38
16 Stabilizing and performance subset .....	40
17 $f(\omega)$ plot for determining admissible $K_p$ range .....	41
18 Entire PID controller sets for $PM = 22.5^\circ$ .....	42
19 Entire PID controller sets for $PM = 30^\circ$ .....	42

FIGURE	Page
20 Entire PID controller sets for $PM = 45^\circ$ .....	43
21 Bode plot of the Example IV.1 plant .....	50
22 Nyquist plot of the Example IV.1 plant .....	51
23 $f(\omega)$ plot for the admissible $K_p$ range about $\theta = [0, 2\pi)$ .....	52
24 $K_d, K_i$ gain set for 12 discrete $\theta$ values in $[0, 2\pi)$ and their intersect area in blue .....	55
25 $K_d, K_i$ gain set for $H_\infty$ constraint, $\gamma = 2$ , when $K_p = 70$ .....	56
26 Bode plot of the plant .....	57
27 Nyquist plot of the plant .....	57
28 Entire $K_i, K_d$ gain for $H_\infty$ constraint, $\gamma = 1$ .....	58
29 Entire $K_i, K_d$ gain for $H_\infty$ constraint, $\gamma = 2$ .....	59
30 Entire PID controller gain sets for $H_\infty$ constraint, $\gamma = 1$ .....	60
31 Bode diagram with upper bound and lower bound of uncertainties .....	66
32 Nyquist plot with uncertainties' boundaries .....	66
33 Bode diagram of the plant .....	68
34 Nyquist diagram of the plant .....	68
35 $f(\omega)$ for illustrating admissible $K_p$ range .....	69
36 Entire robust performance PID gain set for $K_p = 70$ .....	71
37 Bode diagram of compensated sys. with $K_d = 50$ , $K_p = 70$ and $K_i = 16.25$ .....	72
38 Comparison of each step response .....	72
39 Entire robust performance PID gain set for $K_p = 3$ .....	75

## CHAPTER I

### INTRODUCTION

The synthesis of fixed structure controllers for a linear time invariant plant is an open problem with a wide variety of practical applications. Some of the widely used fixed structure controllers are the Proportional Integral Derivative (PID) controllers and the lead-lag controllers. The PID and lead-lag controllers are simple as well as effective and more than half of the industrial applications in use today utilize PID or modified PID control schemes [1]. Despite their wide applicability, the synthesis of PID controllers has not been rigorously solved until recently [2].

The existing systematic methods for the synthesis of PID and fixed structure controllers, with a few notable exceptions, rely on the availability of a mathematical model of the plant. The most notable classical method and exception to synthesize a PID controller is Ziegler-Nichols [3]. A significant feature of this method is its reliance only on empirical data from the plant. It makes an assumption concerning the structure and provides a simple way to compute the proportional, integral and derivative gains from the empirical data. The method is not as effective when the assumed structure of the plant differs significantly from the actual structure. Another significant drawback of the Zeigler-Nichols method is that only one controller set is obtained. This may not satisfy other performance specifications that one may have for a given application.

---

The journal model is *IEEE Transactions on Automatic Control*.

Techniques for synthesizing the sets of stabilizing controllers directly from the empirical data of the plant have not been pursued vigorously until recently. The work of Bhattacharyya and Keel [4] deals with the synthesis of PID and first order controllers when the frequency response of the plant is known over the entire frequency range. The work of Malik *et. al* [5] synthesizes stabilizing controllers of fixed order based on empirical frequency response data at a finite set of frequencies and makes assumptions about the structure of the plant at higher frequencies. The work of Bhattacharyya and Keel [2], [4] also deals with synthesizing sets of PID and lead-lag controllers that guarantee a specified performance while this is not the case with the work of Malik *et. al*. Noise in sensing and measurement is accounted for in the synthesis of fixed order controllers considered by Malik *et. al* [5]. It is a very practical implementation, because the information from the plant such as the magnitude of frequency response may not be exact but coarse to use for an empirical data may be corrupted by noise. This thesis generalizes the work of Bhattacharyya and Keel [4] by accounting for noise in empirical frequency response data in the synthesis of PID and first order controllers. The method proposed here also requires some crude information about the plant such as the relative degree and non-minimum phase zero.

The underlying assumption of the work is that the plant is stable but the performance of the plant is not satisfactory. This is a practical problem which can arise in a variety of situations. For example, any control apparatus bought from a vendor is usually stable and the performance may not be satisfactory. However, it is usually easy to acquire frequency response data for such an apparatus. In this situation, one faces the

following dilemma – whether to obtain a mathematical model for the apparatus or whether to synthesize a controller directly from the acquired data. The latter is a reasonable option especially when the apparatus is given as a black box and when the response seems linear. It is for the latter situation that this thesis addresses.

In particular, it is shown in this thesis how one can compute the sets of stabilizing controllers that guarantee a certain performance specification is met. The performance specifications considered in this work are phase margin and maximum complementary sensitivity function of the closed loop with/without consideration of the uncertain frequency measurement of the system.

The developed algorithms have been implemented in MATLAB<sup>®</sup> and a graphical user interface is provided so that one can plot and verify the set of controllers guaranteeing the specified performance.

#### A. Objective

This research aims to explore a new synthesizing PID and fixed structured controller gains and to verify its reasonableness with the commonly used simple but elaborated theory in order to

- Guarantee the given performance specifications such as the phase margin and/or  $H_\infty$  norm of the sensitivity transfer function for the linear time invariant system.
- Determine the entire set given the frequency response of a continuous LTI system.

- Attain the robustness enhancement of the design for the system from the measured uncertain data.

The basic idea of the above was introduced in [5]. The computation is implemented by MATLAB<sup>®</sup> simulation for the software is widely used in both the academic area and the industry.

## B. Organization of Thesis

In the following part of this thesis many topics will be covered. In Chapter II, earlier results are concerned with mathematical preliminaries such as the Hermite-Biehler theorem, the Mikhailov's plot, as well as the concept of signature of a polynomial for the generalized Hermite-Biehler theorem. Since this research highly concentrates on the performance attainment, only a complex polynomial which is a more general case is handled in Chapter II. Chapters III and IV deal with synthesis of the set of PID controllers that achieve various performance specifications. In Chapter III, achieving the entire set for the given phase margin is introduced and specifically described. Chapter IV provides  $H_\infty$  norm constraint specification, which is analogous to the one shown in Chapter III, and present relevant illustrative examples comparing the stabilizing set. Chapter V studies the robustness property to ensure the proper performance against the estimation error. This is also accomplished in a similar way to the method of Chapter III and IV; however, it employs a series of non-linear inequalities (so called Cone Program). Finally, the contributions of this thesis are summarized in Chapter VI and a few concluding remarks on possible directions for future research are discussed.

## CHAPTER II

### MATHEMATICAL PRELIMINARIES

#### A. Introduction

In this chapter, the mathematical preliminaries are briefly introduced for better understanding the whole later chapters. They have been already employed for PID controller synthesis [5], but they were real polynomial cases having different characteristics against the complex polynomial case. Because this research deals with performance specification which involves  $e^{j\theta}$  in the characteristic polynomial, this chapter describes only the complex polynomial case – more general case rather than the real polynomial one. The real cases of Mikahilov's Criterion and Hermite-Biehler Theorem are well introduced and developed in [2], [4], [5], which one may take a look at for the detail. This chapter is introducing some results for complex case from [5], utilizing these concepts and applying them to the complex cases for the Mikhailov's criterion in section B and the Hermite-Biehler Theorem in section C. In section D, the Hermite-Biehler theorem is generalized for non-Hurwitz polynomial in complex case as well. This generalization plays very important role in this research to define the constraints for confining controller gain convex area, so it is referred and used for later whole chapters to get stabilizing controller set. Next, the algorithm for automatic sign assignment is introduced since this research aims to develop computer aided graphical tool getting PID gain set.

## B. Mikhailov's Criterion

A Hurwitz stable polynomial means that it has all the roots in the left half (LHP) of the complex plane. In order for the stability of a system, this Hurwitz condition is required mathematically. For a Hurwitz stable complex polynomial  $P(s)$ , the Mikhailov's criterion states that the polynomial  $P(s)$  is Hurwitz if and only if the frequency response plot (plot of  $P(j\omega)$ ) starts on any specific quadrant and passes through exactly  $2n$  quadrants in the counterclockwise direction as  $\omega$  increases from  $-\infty$  to  $\infty$ , where  $n$  is the degree of the polynomial [5].

**Lemma II.1.** Let  $P(j\omega) = P_r(\omega) + jP_i(\omega)$ .  $P_r(\omega)$  and  $P_i(\omega)$  are polynomials with real coefficients. It is observed that  $P_r(\omega)$  and  $P_i(\omega)$  have same degree of  $n$ . The starting quadrant can be found as

- If the leading coefficient of  $P_r(\omega)$  and  $P_i(\omega)$  are of the same sign, then  
Mikhailov's plot starts in the first or third quadrant at  $\omega = -\infty$
- If the leading coefficient of  $P_r(\omega)$  and  $P_i(\omega)$  are of the different sign, then  
Mikhailov's plot starts in the second or fourth quadrant at  $\omega = -\infty$

In Fig. 1 Lemma II.1 is well illustrated for Hurwitz complex polynomial.

Consider following Example II.1.



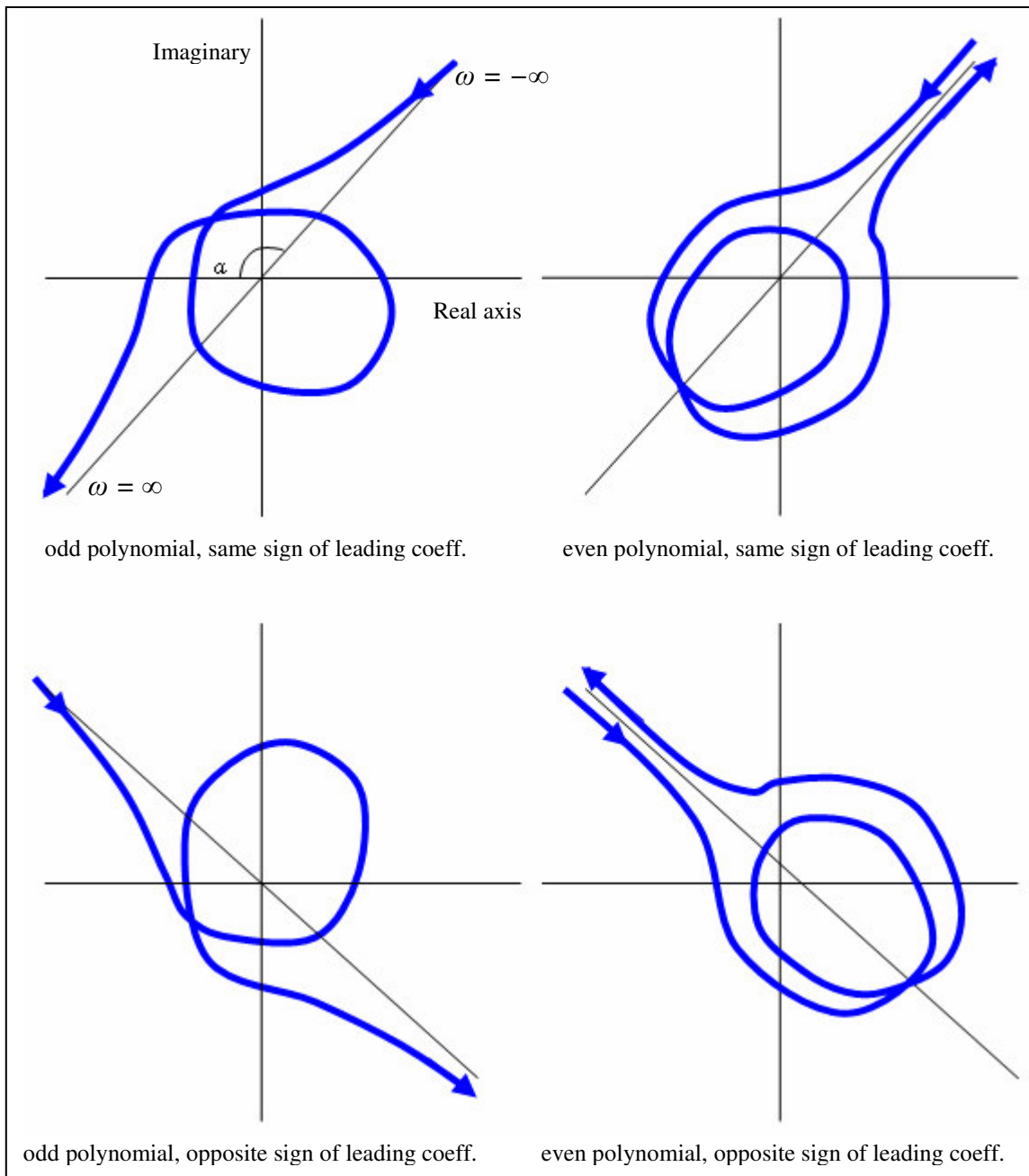


Fig. 1. Mikhailov's plot for Hurwitz complex polynomial

**Example II.1.** Consider the given complex Hurwitz polynomial  $P(s)$

$$P(s) = (1 - j)s^3 + (7 - j)s^2 + (26 - 7j)s + 36 - 2j \quad (2.1)$$

and  $P(j\omega)$  can be decomposed into the real part and the imaginary part as

$$\begin{aligned} P(j\omega) &= P_r(\omega) + j P_i(\omega) \\ &= (-\omega^3 - 7\omega^2 + 7\omega + 36) + j(-\omega^3 + \omega^2 + 26\omega - 2) \end{aligned} \quad (2.2)$$

As seen in Fig. 2, the Mikhailov's plot of the given complex polynomial starts on 1<sup>st</sup> quadrant and turns in the counterclockwise direction going through  $2n = 6$  ( $n = 3$ ) quadrants as  $\omega$  goes from  $-\infty$  to  $\infty$ . It is noted that the plot in the extreme frequency region has an inclination which depends on the each part of leading polynomial's coefficient,  $45^\circ$  ( $= \tan^{-1}\left(\frac{-1}{-1}\right)$ ) here. Furthermore, it is observed that the net change in phase as  $\omega$  proceeds from  $-\infty$  to  $\infty$  is  $3\pi$ . In general for a Hurwitz stable polynomial, this net change is  $n\pi$ , where  $n$  is the degree of the polynomial [6].

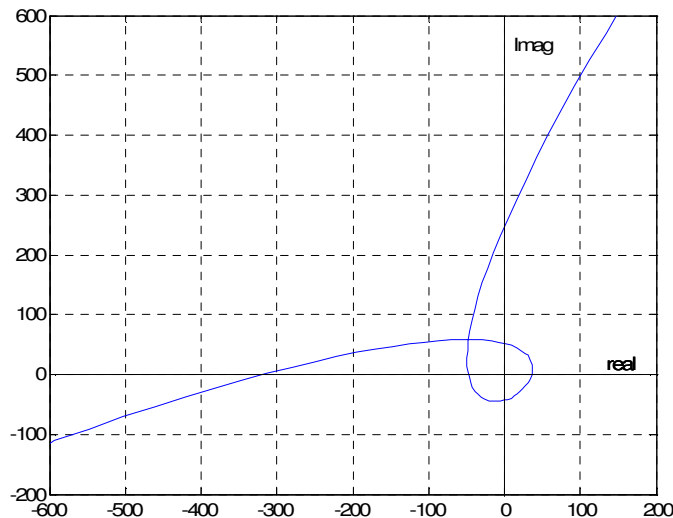


Fig. 2. Mikhailov's plot for Example II.1

### C. Hermite-Biehler Theorem for Complex Polynomials

We continue the discussion over the complex polynomial,  $P(s)$  as shown in the previous section. The Hermite-Biehler theorem gives a necessary and sufficient condition for a given polynomial to be stable. The theorem says that the polynomial  $P(s)$  is Hurwitz if and only if all roots  $P_r(\omega)$  and  $P_i(\omega)$  are real and interlace according to the following [5]:

#### Lemma II.2.

- If the leading coefficient of  $P_r(\omega)$  and  $P_i(\omega)$  are of the same sign, then

$$-\infty < \omega_{r1} < \omega_{i1} < \omega_{r2} < \omega_{i2} < \dots < \omega_m < \omega_{in} < \infty$$

- If the leading coefficient of  $P_r(\omega)$  and  $P_i(\omega)$  are of the different sign, then

$$-\infty < \omega_{i1} < \omega_{r1} < \omega_{i2} < \omega_{r2} < \dots < \omega_{in} < \omega_m < \infty$$

The proof of the Hermite-Biehler Theorem for complex polynomials is an extension version of the real case, which can be found in [2]. Consider the following example.

**Example. II.2.** Reconsider the same polynomial from example II.1. The roots of each decomposed polynomial can be found as

$$P_r(\omega) = -\omega^3 - 7\omega^2 + 7\omega + 36$$

$$P_i(\omega) = -\omega^3 + \omega^2 + 26\omega - 2$$

$$P_r(\omega)=0 : \omega_r = -7.2824, -2.0867, 2.3691$$

$$P_i(\omega)=0 : \omega_i = -4.6651, 0.0767, 5.5884 \quad (2.3)$$

which shows the interlacing property of Hermite-Biehler theorem well in Fig. 3. Again, this property shows  $P(s)$  in Example. II.1 is indeed Hurwitz.

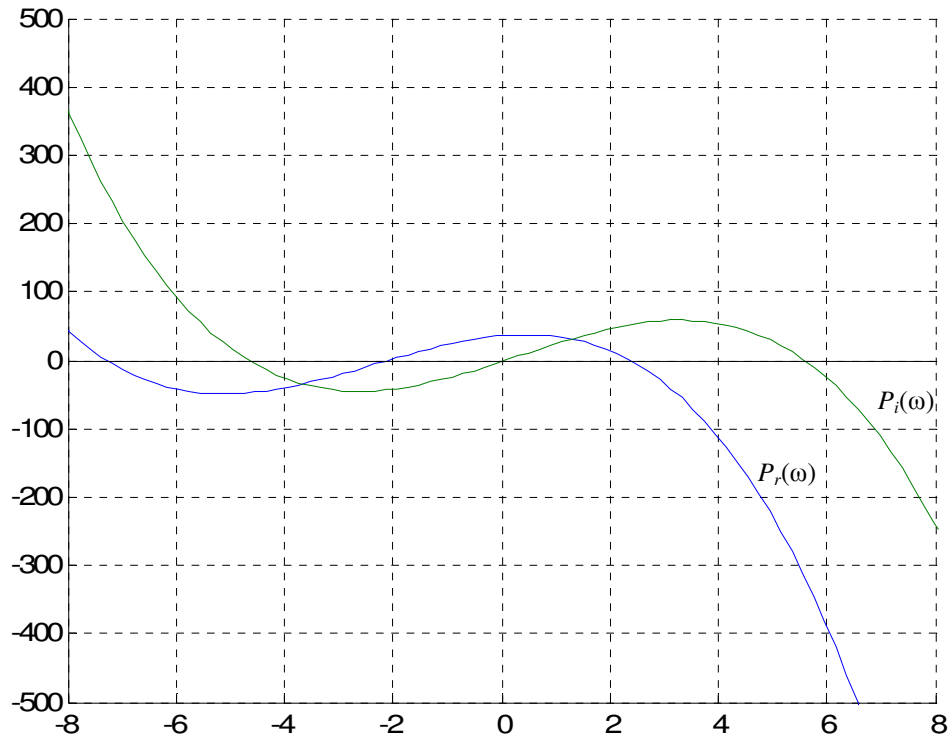


Fig. 3. Interlacing property for a Hurwitz polynomial

#### D. Generalization of the Hermite-Biehler Theorem

As shown in the previous section, the Hermite-Biehler theorem is valid for only polynomials which are Hurwitz. The Generalization of the Hermite-Biehler theorem is used for not necessarily Hurwitz polynomials. In this section the complex polynomial is also handled for applying Generalization of the theorem.

In [2] Bhattacharyya *et. al.* introduced the lemma of the generalization of the Hermite-Biehler theorem for real polynomials to show a relationship between the net accumulated phase of  $P(j\omega)$  and the difference between the numbers of roots of the

polynomials in LHP and RHP. The relationship for complex polynomials can be deemed in a similar way to that of real polynomials as following lemma:

**Lemma II.3.** For a given complex polynomial  $P(s)$  with no imaginary axis roots, let  $l(P)$  and  $r(P)$  denoted the number of left and right half zeros in the complex plane. Let  $\angle\Delta_{-\infty}^{\infty}\theta$  denote the total change in phase of  $P(j\omega)$  as  $\omega$  goes from  $-\infty$  to  $\infty$ .

Then,

$$\angle\Delta_{-\infty}^{\infty}\theta = \pi\{l(P) - r(P)\} \quad (2.4)$$

**Proof** In general it is noted that the roots in the left half of the complex plane ( $l(P)$ ) contribute  $\pi$  while the roots on the right half of the complex plane ( $r(P)$ ) contribute  $-\pi$  to the net change in phase. □

Now, in order to examine the total phase change of  $P(j\omega)$ , we need to decompose  $P(j\omega)$  into  $P_r(j\omega)$  and  $P_i(j\omega)$ , where  $P_r$  and  $P_i$  are all real polynomials as

$$P(j\omega) = P_r(\omega) + jP_i(\omega) \quad (2.5)$$

Let

$$\text{sgn}[x] = \begin{cases} +1 & \text{if } x > 0 \\ -1 & \text{if } x < 0 \\ 0 & \text{if } x = 0 \end{cases} \quad (2.6)$$

The total phase change of  $P(j\omega)$ ,  $\angle\Delta_{-\infty}^{\infty}P(j\omega)$ , now can be calculated below, which result is very similar way to that derived by the work of Bhattacharyya *et. al.* [2].

**Theorem II.1.** Let the distinct real roots of imaginary part of polynomial,  $P_i(\omega) = 0$  denote

$$-\infty < \omega_1 < \omega_2 < \dots < \omega_{l-1} < \omega_l < \infty$$

And assume that there is at least one more real roots of  $P_r(\omega)$ , then signature of the polynomial  $l(P) - r(P)$  which means the difference of numbers between LHP roots and RHP roots and is symbolized as  $\sigma$ , is given by

$$\begin{aligned} \sigma(P) &= l(P) - r(P) = \frac{1}{\pi} \angle \Delta_{-\infty}^{\infty} P(j\omega) \\ &= d(-1) \cdot 1 + \frac{1}{2} \operatorname{sgn}[\dot{P}_i(\omega_1)] \{ \operatorname{sgn}[P_r(\omega_1)] - 2 \operatorname{sgn}[P_r(\omega_2)] + 2 \operatorname{sgn}[P_r(\omega_3)] \\ &\quad \dots + 2(-1)^{l-2} \operatorname{sgn}[P_r(\omega_{l-1})] + (-1)^{l-1} \operatorname{sgn}[P_r(\omega_l)] \} \end{aligned} \quad (2.7)$$

where  $d$  stands for the direction that the Mikailov's plot rotates in the axis of the origin.

When the plot rotates in counter-clockwise direction,  $d$  is 1, otherwise  $d$  is  $-1$ . It is also observed that when  $d$  is 1, the first root appearance in Lemma II.1 is holding, but when  $d$  is  $-1$ , it is opposite.

**Proof.** When  $\omega$  travels from  $-\infty$  to  $\infty$ , the roots in LHP contribute  $l(P) \cdot \pi$  and the roots in RHP does  $r(P) \cdot \pi$ . Hence, the total phase change of  $P(j\omega)$  can be easily obtained by

$$\angle \Delta_{-\infty}^{\infty} P(j\omega) = \{l(P) - r(P)\} \pi = \sigma(P) \pi \quad (2.8)$$

The change in the phase of  $\delta(j\omega)$  from  $\omega_k$  to  $\omega_{k+1}$  is given by:

$$\frac{\pi}{2} \operatorname{sgn}[\dot{P}_i(\omega_k)] \{ \operatorname{sgn}[P_r(\omega_k)] - \operatorname{sgn}[P_r(\omega_{k+1})] \} \quad (2.9)$$

So the total phase change of  $P(j\omega)$  can be shown by

$$\begin{aligned}
\angle \Delta_{-\infty}^{\infty} P(j\omega) &= d(-1)\alpha + \frac{\pi}{2} \left\{ \operatorname{sgn} \left[ \frac{P_i(\omega_1)}{d\omega} \right] (\operatorname{sgn}[P_r(\omega_1)] - \operatorname{sgn}[P_r(\omega_2)]) \right. \\
&+ \operatorname{sgn} \left[ \frac{P_i(\omega_2)}{d\omega} \right] (\operatorname{sgn}[P_r(\omega_2)] - \operatorname{sgn}[P_r(\omega_3)]) \\
&+ \operatorname{sgn} \left[ \frac{P_i(\omega_3)}{d\omega} \right] (\operatorname{sgn}[P_r(\omega_3)] - \operatorname{sgn}[P_r(\omega_4)]) \\
&\quad \dots \dots \\
&\left. + \operatorname{sgn} \left[ \frac{P_i(\omega_{l-1})}{d\omega} \right] (\operatorname{sgn}[P_r(\omega_{l-1})] - \operatorname{sgn}[P_r(\omega_l)]) \right\} + d(-1)(\pi - \alpha) \tag{2.10}
\end{aligned}$$

where  $\alpha$  is the inclination angle that the Mikhailov's plot converges when  $\omega \rightarrow \infty$  or  $-\infty$ .

It is noted that the angle,  $d(-1)\alpha$  ( $0 < \alpha < \pi$ ), inherently represents the phase change from  $\omega = -\infty$  to  $\omega = \omega_l$  in the above equation. When the phase change from  $-\infty$  to  $\omega_l$  is  $\alpha$ , the phase change from  $\omega_l$  to  $\infty$  is specified by  $d(-1)(\pi - \alpha)$ .

Since  $\operatorname{sgn}[\dot{P}_i(\omega_{k+1})] = -\operatorname{sgn}[\dot{P}_i(\omega_k)]$ , the phase change in  $P(j\omega)$  from  $\omega = -\infty$  to  $\omega = \infty$  can be compressed by

$$\begin{aligned}
\angle \Delta_{-\infty}^{\infty} P(j\omega) &= d(-1)\pi + \frac{\pi}{2} \operatorname{sgn}[\dot{P}_i(\omega_1)] (\operatorname{sgn}[P_r(\omega_1)] - 2\operatorname{sgn}[P_r(\omega_2)] + 2\operatorname{sgn}[P_r(\omega_3)] \\
&\quad \dots \dots + 2(-1)^{l-2} \operatorname{sgn}[P_r(\omega_{l-1})] + (-1)^{l-1} \operatorname{sgn}[P_r(\omega_l)]). \tag{2.11}
\end{aligned}$$

Therefore, we relate (2.8) and (2.11), then obtain

$$\sigma(P(j\omega)) = d(-1) + \frac{1}{2} \operatorname{sgn}[\dot{P}_i(\omega_1)] (\operatorname{sgn}[P_r(\omega_1)] - 2\operatorname{sgn}[P_r(\omega_2)] \dots (-1)^{l-1} \operatorname{sgn}[P_r(\omega_l)]) \tag{2.12}$$

which is, indeed, identical to (2.7). □

Consider the following example

**Example II.3.**

$$P(s) = (4.4496 + 0.3092 j)s^5 + (2.4708 - 1.7198 j)s^4 + (-3.4447 - 3.6099 j)s^3 + (-0.5903 - 3.5781 j)s^2 + (0.1032 - 1.9176 j)s + (-0.8766 - 0.2178 j) \quad (2.13)$$

As seen from the obtained roots, there are 2 roots in LHP and 3 roots in RHP. It is noted that the Mikahilov's plot passes through only 4 quadrants in Figs. 4 and 5, and it should go through 10 ( $2 \cdot 5 = 10$ ) quadrants, if it were Hurwitz. And the interlacing property is not met in Fig. 6, which is magnified in Fig. 7, hence it is confirmed that the polynomial in this example is not Hurwitz by the Hermite-Biehler theorem.

$$P_r(\omega) = -3092s^5 + 24708s^4 - 36099s^3 + 5903s^2 + 19176s - 8766$$

$$P_i(\omega) = 44496s^5 - 17198s^4 + 34447s^3 + 35781s^2 + 1032s - 2178$$

$$P_r(\omega)=0: \text{real}(\omega_r) = -0.7057, 0.5956, 6.1746.$$

$$P_i(\omega)=0: \text{real}(\omega_i) = -0.4348, -0.3817, 0.2139. \quad (2.14)$$

By Theorem II.1,

$$\begin{aligned} l(P) - r(P) &= \frac{1}{\pi} \angle \Delta_{-\infty}^{\infty} P(j\omega) = -1 + \frac{1}{2} \text{sgn}[\dot{P}_i(\omega_1)] [\text{sgn}[P_r(\omega_1)] - 2 \text{sgn}[P_r(\omega_2)] + \text{sgn}[P_r(\omega_3)]] \\ &= -1 + \frac{1}{2} \cdot 1 \cdot (-1 - 2 \cdot -1 + -1) = -1 \quad (d = -1) \end{aligned} \quad (2.15)$$

Indeed, the roots for this non-Hurwitz complex polynomial are

$$\begin{aligned} \text{roots} &= 1.0619 + 0.6392j, \\ &0.0732 - 0.6585j, \\ &-0.9231 + 0.1154j, \\ &-0.8378 + 0.0270j, \\ &0.1000 + 0.3000j \end{aligned} \quad (2.16)$$



which gives  $l(P) - r(P) = 2 - 3 = -1$

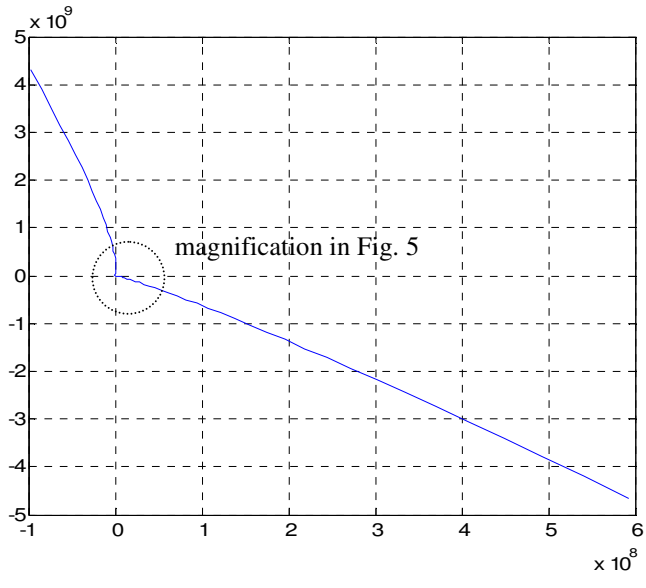


Fig. 4. Mikhailov's plot

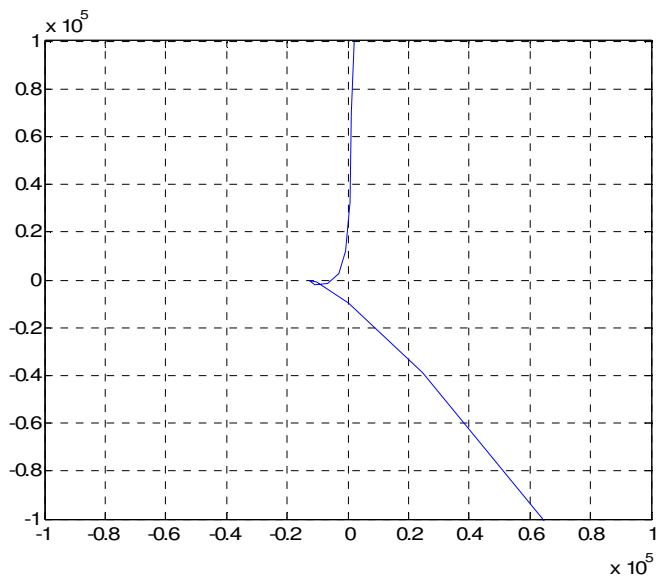


Fig. 5. Magnified Mikhailov's plot of Fig.3.

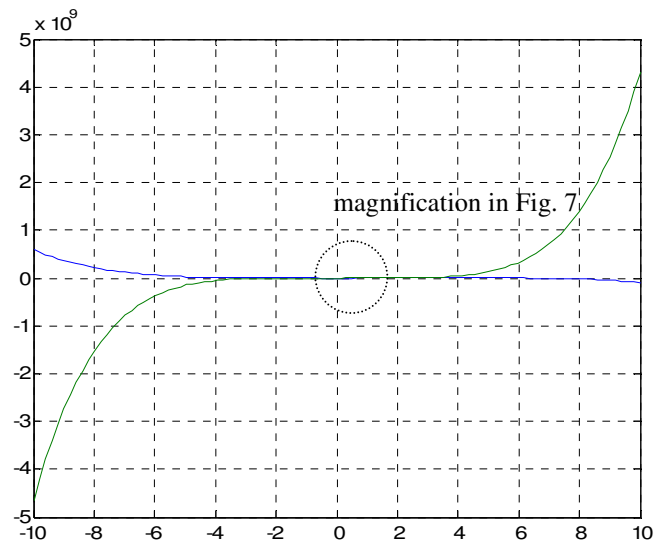


Fig. 6. Decomposition into real and imaginary part

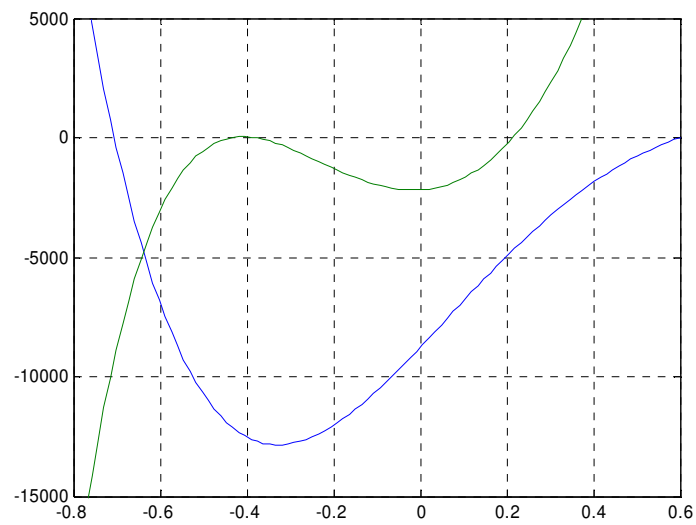


Fig. 7. Magnification of Fig. 6.

### E. Algorithm for Automatic Sign Assignment

In this section, the algorithm for giving all the possible sign sets is studied when there exist more real roots than the least required roots that will be discussed in Chapter III and used in following chapters. The algorithm is to be developed for systematical computation when  $l$  is arbitrary number of roots and more than  $r$  (required number of roots by the generalized Hermite-Biehler theorem).

For the background, it is noted that

$${}_n C_r = \frac{{}_n P_r}{r!} = \frac{n!}{r!(n-r)!} \quad (2.17)$$

The generalized Hermite-Biehler theorem can be shown as

$$i_1 - 2i_2 + 2i_3 \cdots + 2(-1)^{l-2}i_{l-1} + (-1)^{l-1}i_l = 2(r-1), \quad i_k = 1 \text{ or } -1 \quad (2.18)$$

**Proposition II.1.** The number of sets  $S$  can be determined by

when  $l - r$  is even,

either  $i_1$  and  $i_l$  should be +1 or  $i_1$  and  $i_l$  should be -1, thus

$$S = {}_{l-2} C_{Q\left(\frac{l-r}{2}\right)} + {}_{l-2} C_{\left(Q\left(\frac{l-r}{2}\right)-1\right)} \quad (2.19)$$

when  $l - r$  is odd

either  $i_1$  and  $i_l$  be +1 and -1 or -1 and +1, thus

$$S = 2 \cdot {}_{l-2} C_{Q\left(\frac{l-r}{2}\right)} \quad (2.20)$$

where  $Q\left(\frac{l-r}{2}\right)$  stands for the quota of  $\frac{l-r}{2}$ .

**Proof.** Let  $p(i_k)$  and  $q(i_k)$  denote

$$p(i_k) = i_1 + (-1)^{l-1} i_l \quad (k = 1, l),$$

$$q(i_k) = -2i_2 + 2i_3 \cdots + 2(-1)^{l-2} i_{l-1}, \quad (k = 2, 3, \dots, l-1)$$

First, we need to compare the parities in each side of (2.18) and make them matched. When  $l-r$  is even, both  $l$  and  $r$  have same parity. Because  $r-1$ 's parity becomes different from  $r$  and  $q(i_k)/2$  is always same parity to that of  $l$ ,  $p(i_k)$  should contribute 2 by that the first and last term ought to be added to match the parities in equation (2.13) divided 2. On the other hand, when  $l-r$  is odd,  $l$  and  $r$  have always different parity. Similarly, because  $r-1$ 's parity is changed from that of  $r$ , so  $p(i_k)$  should be 0 so that  $q(i_k)/2$  should be remained as same parity to that of  $l$ . Thus, when  $l-r$  is odd, the first and last term should be subtracted to match the parities likewise.

Second, it is necessary to remove redundant number of roots. We only need to consider  $q(i_k)$  at this step and determine how many redundancies should be. The total number of terms in  $q(i_k)$  is  $l-2$  and if we select  $n$  number of terms as a result of  $-1$ , then  $2n$  number of terms are to be subtracted. The redundancies can be calculated by

$$\text{when } l-r \text{ is even, } l-2+1-(r-1) = l-r \quad (2.21)$$

$$\text{when } l-r \text{ is odd, } l-2-(r-1) = l-r-1 \quad (2.22)$$

Therefore, there are possibilities that  $-1$  term in  $q(i_k)$  can be chosen as many as

$$Q\left(\frac{l-r}{2}\right) \text{ among } l-2 \text{ number of terms.} \quad \square$$

**Example II.4.**

a. Suppose  $l = 4$  and  $r = 2$ , then the possibilities can be determined by

$${}^{4-2}C_{\varrho\left(\frac{4-2}{2}\right)} + {}^{4-2}C_{\varrho\left(\frac{4-2}{2}\right)-1} = {}_2C_1 + {}_2C_0 = 2 + 1 = 3. \quad (2.23)$$

$$i_1 - 2i_2 + 2i_3 - i_4 = 2(2-1) = 2 \quad (2.24)$$

$$\begin{aligned} F^* &= \{ i_1, i_2, i_3, i_4 \} = \{ 1, -1, -1, -1 \} \\ &= \{ 1, 1, -1, -1 \} \\ &= \{ -1, -1, 1, 1 \} \end{aligned} \quad (2.25)$$

b.  $l = 6$  and  $r = 3$ , then the possibilities can be found by  ${}^{2 \cdot 6-2}C_{\varrho\left(\frac{6-3}{2}\right)} = {}_4C_2 = 12$ . (2.26)

$$i_1 - 2i_2 + 2i_3 - 2i_4 + 2i_5 - i_6 = 2(3-1) = 4 \quad (2.27)$$

$$\begin{aligned} F^* &= [\{ i_1, i_2, i_3, i_4, i_5, i_6 \}] = [ \{ 1, 1, -1, -1, 1, 1 \}, \\ &\quad \{ 1, 1, 1, 1, 1, 1 \}, \\ &\quad \{ 1, 1, 1, -1, -1, 1 \}, \\ &\quad \{ 1, -1, -1, 1, 1, 1 \}, \\ &\quad \{ 1, -1, -1, -1, -1, 1 \}, \\ &\quad \{ 1, -1, 1, 1, -1, 1 \}, \\ &\quad \{ -1, 1, -1, -1, 1, -1 \}, \\ &\quad \{ -1, 1, 1, 1, 1, -1 \}, \\ &\quad \{ -1, 1, 1, -1, -1, -1 \}, \\ &\quad \{ -1, -1, -1, 1, 1, -1 \}, \\ &\quad \{ -1, -1, -1, -1, -1, -1 \}, \\ &\quad \{ -1, -1, 1, 1, -1, -1 \} ] \end{aligned} \quad (2.28)$$

Next, an algorithm for making systematic Combination function ( ${}_nC_r$ ) is introduced. In this research, we need a Combination function making every possible combinations automatically with given  $r$  choosing number in the  $n+1/-1$  pool. Consider the case that  $r$  piece of  $-1$ s are selected among  $n$  tuples, which is expressed by  ${}_nC_r$  as shown below.

$$\begin{aligned}
 {}_nC_r = & \{ \underbrace{-1, -1, \dots, -1}_r, +1, \dots, +1, +1 \} \\
 & \underbrace{\hspace{10em}}_n \\
 & \vdots \\
 & \{ +1, \dots, +1, +1, -1, -1, \dots, -1 \}
 \end{aligned} \tag{2.29}$$

The basic idea implemented in this algorithm is a counter's working logic that at each event a bit is added from LSB (the least significant bit) to MSB (the most significant bit).

$\{-1, -1, \dots, -1, +1, \dots, +1, +1\}$  is corresponding to its address

$$\begin{array}{c}
 [000 \dots 00] \\
 \uparrow \quad \quad \quad \uparrow \\
 \text{LSB} \quad \quad \quad \text{MSB}
 \end{array} \tag{2.30}$$

- Step 1. Generate  $-1$ 's address as many as the number of  $-1$
- Step 2. Start adding 1 from LSB at each step
- Step 3. Find any count to be  $n - r$  or whether the sum of all is to be  $n - r$ .

If so, then initialize all the lower digits behind it and add 1 to upper digit

- Step 4. Finish it when MSB becomes  $n - r$ , otherwise go to step 2.

In step 1, the address tells where each  $-1$  is located in any combination. LSB stands for right-most one and MSB left-most one in combination. Address value means

the number of +1 in front of any -1. For instance, the combination, { -1, +1, -1, +1, -1 }, is corresponding to the address, [ 0 1 1].

In step 2, at each sequence add 1 at LSB of the address. This is analogous to that of a digital counter.

In step 3, compare each step's status with the condition that any count digit is equivalent to  $n - r$  or the sum of all digits is  $n - r$ . If that condition is met, digit value is carried into higher level to MSB and initialized lower level digits until LSB.

In step 4, refer MSB and if it becomes  $n - r$ , then the program is terminated. Otherwise, go to step 2 and repeat all the procedure.

**Example II.5.** Find corresponding address to each combination of sign for  ${}_5C_3$ .

Combination	:	Address	
${}_5C_3 = \{-1, -1, -1, 1, 1\}$	:	[ 0 0 0 ]	
$\{-1, -1, 1, -1, 1\}$	:	[ 1 0 0 ]	
$\{-1, -1, 1, 1, -1\}$	:	[ 2 0 0 ]	
$\{-1, 1, -1, -1, 1\}$	:	[ 0 1 0 ]	
$\{-1, 1, -1, 1, -1\}$	:	[ 1 1 0 ]	
$\{-1, 1, 1, -1, -1\}$	:	[ 0 2 0 ]	
$\{1, -1, -1, -1, 1\}$	:	[ 0 0 1 ]	
$\{1, -1, -1, 1, -1\}$	:	[ 1 0 1 ]	
$\{1, -1, 1, -1, -1\}$	:	[ 0 1 1 ]	
$\{1, 1, -1, -1, -1\}$	:	[ 0 0 2 ]	(2.31)

## CHAPTER III

### FIXED STRUCTURE CONTROLLER SYNTHESIS FOR PHASE MARGIN PROPERTY

#### A. Introduction

Since the controller should be reliant in the real world system through any unpredictable events, the gain margin and phase margin take very important part in the control synthesis theory to examine how much stable the system is [7]. In this chapter, the phase margin is only taken into consideration for this objective, since it has a more meaningful study reason rather than the gain margin which can be achieved by small effort. The phase margin case is more difficult than the gain margin one, because the former is involved in complex polynomial analysis in order to get the sign signature for the stability of the system. On the other hand, the latter has a real polynomial, which is just the same case with stabilizing synthesis theory without considering performances. In [8], [9] the performance evaluation including phase margin has been achieved, however, the calculation went through iteration of several testing points with given limited  $K_d$ ,  $K_i$  stabilizing area from fixed  $K_p$  gain value, which requires far more computational time than using the algorithm proposed here. Furthermore, the result from iteration can not be exact for complete controller set satisfying given performance criteria, because only a few points were tested from repetition of evaluating performance specifications. The main purpose of this chapter is to develop algorithm for assessing given performance



factors in section B. Applying this algorithm, in section C, the satisfying performance sets are determined not from an accurate analytical model of the plant but from an empirical data of the plant in terms of its frequency response and physical considerations.

## B. Theory and Algorithm

This section introduces a theory for synthesizing a rational, proper stabilizing PID controller  $C(s)$  satisfying given phase margin, such that the polynomial  $D_c(s)$  of degree 2 and the polynomial  $N_c(s)$  of degree 2 are shown by (3.1).

$$C(s) = \frac{N_c(s)}{D_c(s)} = \frac{K_i + K_p s + K_d s^2}{s + Ts^2} \quad (3.1)$$

The coefficient  $T$  is a very small positive number such as  $10^{-4}$  and is put to enable the controller  $C(s)$  to be handled as a proper rational transfer function. Let  $K$  be the vector of controller coefficients:

$$K = [ K_i \ K_p \ K_d ]^T \quad (3.2)$$

The determination of the vector  $K$  - controller coefficients - is equivalent to that of the stabilizing controller  $C(s)$ . The main objective is to guarantee a phase margin of  $\phi$  for a SISO plant, the following criterion [5] is used in this chapter so as to be Hurwitz.

**Lemma III.1 [5].**

$$\Delta(s) = D_p(s)D_c(s) + e^{j\theta} N_p(s)N_c(s) \quad (3.3)$$

where a transfer function  $H_p(s) = \frac{N_p(s)}{D_p(s)}$  is stabilized by a fixed order controller,

$$C(s) = \frac{N_c(s)}{D_c(s)} \text{ for every } \theta \in (-\phi, \phi).$$

Furthermore, as mentioned earlier, we make use of only empirical data in terms of its frequency response from the plant. Hence, the above criterion (3.3) must be revised into the rational function,  $\delta(s)$ , as shown below.

$$\delta(s) = \Delta(s) \frac{N_p(-s)}{D_p(s)D_p(-s)} \quad (3.4)$$

If  $\Delta(s)$  has coefficients that are affine in the controller coefficients, then the rational function,  $\delta(s)$ , is also affine in the controller coefficients [5]. In order to proceed applying the mathematical preliminaries shown in Chapter II to this rational function,  $\delta(s)$ , we have to assume the followings about the plant:

- The transfer function  $H_p(s) = \frac{N_p(s)}{D_p(s)}$  of the plant is stable, rational and strictly proper, which means the degree  $n$  of  $D_p(s)$  is greater than the degree  $m$  of  $N_p(s)$  for some coprime polynomials,  $N_p(s)$  and  $D_p(s)$ .
- The plant does not have any pole and zero on the imaginary axis, i.e.,  $N_p(j\omega) \neq 0$ ,  $D_p(j\omega) \neq 0$ , for  $\omega \in (-\infty, \infty)$ .

The root counting and phase unwrapping of Hurwitz real polynomials is employed for generalization of non-Hurwitz complex polynomials, as shown already in Chapter II, to yield sets of controllers systematically in the parameter space. Again, the polynomial we are considering is complex due to the exponential term,  $e^{j\theta}$  which is aggravating the stability as much as the given phase margin. As far as the total phase accumulation of  $\delta(j\omega)$  is examined as  $\omega$  varies from  $-\infty$  to  $+\infty$ , the generalized Hermite-Biehler theorem can still stand as shown in Theorem III.1. The reason why we

have to examine the phase change from  $-\infty$  to  $+\infty$  is that the complex polynomial's real part roots are not to be symmetry with respect to imaginary axis generally. Now, the generalized Hermite-Biehler theorem in Theorem II.1 is applied to Lemma III.1 for deriving entire phase margin gain sets, leading the following Theorem III.1.

**Theorem III.1.** Consider characteristic rational function;

$$\delta(s) = \Delta(s) \frac{N_p(-s)}{D_p(s)D_p(-s)}, \text{ for } \theta \in (0, \frac{\pi}{2}) \quad (3.5)$$

Let the real roots  $\omega_k$  of  $\delta_i(s)$  be

$$\omega_k = -\infty < \omega_1 < \omega_2 < \omega_3 \cdots \cdots < \omega_{l-1} < \omega_l < \infty$$

Let the sign of  $\delta_r(s)$  at these frequencies denote correspondingly  $i_1, i_2, i_3, \cdots \cdots, i_{l-1}, i_l$ .

Then,  $\Delta(s)$  is Hurwitz if and only if

$$2(n - m + r + 2u - 1) = \text{sgn} \left[ \frac{d\delta_i(\omega_1)}{d\omega} \right] \{i_1 - 2i_2 + 2i_3 \cdots + 2(-1)^{l-2}i_{l-1} + (-1)^{l-1}i_l\} \quad (3.6)$$

In (3.6),  $n$  is the degree of the denominator of the plant,  $m$  is the degree of the numerator of the plant,  $r$  is the degree of the compensator which is 2 and  $u$  is the non-minimum phase zero of the plant.

**Proof.** Note that the degree of the polynomial  $\Delta(s)N_p(-s)$  is  $n + r + m$ . Since the denominator of  $\delta(s)$  does not contribute any angle change, we need to consider the numerator only,  $\Delta(s)N_p(-s)$ . The number of roots of  $N_p(s)$  in LHP is equivalent to  $m - u$ . Similarly, the number of roots of  $N_p(s)$  in RHP is  $u$ . Thus, the number of roots of  $N_p(-s)$  in LHP is  $u$  and the number in RHP is  $m - u$ . Hence, the signature of  $\Delta(s)N_p(-s)$  can be easily obtained by

$$\begin{aligned}\sigma(\Delta(s)N_p(-s)) &= (n+r+u) - (m-u) \\ &= n-m+r+2u\end{aligned}\quad (3.7)$$

Let the sign of  $\frac{d\delta_i(\omega)}{d\omega}$  at  $\omega = \omega_k$  symbolize  $I_k$ . The change in the phase of  $\delta(j\omega)$  from  $\omega_k$

to  $\omega_{k+1}$  is given by:  $I_k(i_k - i_{k+1})\frac{\pi}{2}$ . Since  $I_{k+1} = -I_k$ , the phase change in  $\delta(j\omega)$  from  $\omega =$

$-\infty$  to  $\omega = \infty$  can be expressed as:

$$\Delta_{-\infty}^{\infty}(\delta(\omega)) = \alpha + I_1\{(i_1 - i_2) - (i_2 - i_3) + \dots + (-1)^{l-2}(i_{l-1} - i_l)\}\frac{\pi}{2} + (\pi - \alpha) \quad (3.8)$$

The angle,  $\alpha$  ( $0 < \alpha < \pi$ ), represents the phase change from  $\omega = -\infty$  to  $\omega = \omega_1$  in the above equation. When the phase change from  $-\infty$  to  $\omega_1$  is  $\alpha$ , the phase change from  $\omega_1$  to  $\infty$  is specified by  $\pi - \alpha$ . It is observed in the following section that the degree of both  $\delta_r(j\omega)$  and  $\delta_i(j\omega)$  should be same, because  $H_p(-j\omega)$  is evenly distributed to the real part and the imaginary part of decomposed rational function respectively by  $e^{j\theta}$  term. Thus, the asymptotic angle for  $\omega \rightarrow -\infty$  or  $\rightarrow \infty$  is determined by the leading coefficients of  $\delta_r(j\omega)$  and  $\delta_i(j\omega)$ , simultaneously.

Therefore, from the above, the signature equation (3.7) and the total phase change of  $\delta(j\omega)$  (3.8) are related by

$$(n-m+r+2u)\pi = \alpha + I_1\{(i_1 - i_2) - (i_2 - i_3) + \dots + (-1)^{l-2}(i_{l-1} - i_l)\}\frac{\pi}{2} + (\pi - \alpha) \quad (3.9)$$

Since  $I_l = \text{sgn}\left[\frac{d\delta_i(\omega_l)}{d\omega}\right]$  and  $I_k = (-1)^{k-1} I_l$  from the interlacing property of the rational

function, the change in the phase of  $\delta(j\omega)$  as  $\omega$  changes from  $-\infty$  to  $\infty$  is:

$$(n - m + r + 2u) = \left( \operatorname{sgn} \left[ \frac{d\delta_i(\omega)}{d\omega} \right]_{\omega=\omega_i} \left\{ i_1 - 2i_2 + 2i_3 \cdots + 2(-1)^{l-1}i_{l-1} + (-1)^l i_l \right\} \frac{1}{2} + 1 \right) \quad (3.10)$$

which is identical to (3.6). Note that the accumulation of phase of  $\Delta(j\omega)N_p(-j\omega)$  is equivalent to that of  $\delta(j\omega)$  as  $(n - m + r + 2u) \frac{\pi}{2}$  if and only if  $\Delta(s)$  is Hurwitz.  $\square$

It is noted that we do not have to know the exact  $n$  and  $m$ . The relative degree  $n - m$  can be inferred from the plant transfer function's frequency responses at sufficiently high frequencies. The number of non-minimum phase zeros,  $u$  of the plant also can be found, in some cases, from total phase change of frequency response data.

### C. Determination of Controller Parameter Set

This section describes how the signature condition is utilized to attain the controller gain set for the given performance specifications. First of all, we need to analyze the characteristic rational function,  $\delta(s)$ , into separated form by real part and imaginary part. A derivation of the equation is now presented as follows.

Consider a plant  $H_p(s)$  with the transfer function and the controller  $C(s)$  again

$$H_p(s) = \frac{N_p(s)}{D_p(s)} \quad (3.11)$$

$$C(s) = \frac{N_c(s)}{D_c(s)} = \frac{(K_i + K_p s + K_d s^2)}{s(1+Ts)}, \text{ where } T > 0 \text{ is very small number.} \quad (3.12)$$

The modified characteristic rational function,  $\delta(s)$ , can be shown by

$$\delta(s) = \frac{[N_p(s)N_c(s) + e^{-j\theta}D_p(s)D_c(s)]N_p(-s)}{D_p(s)D_p(-s)} \quad (3.13)$$

Thus to ensure that the characteristic equation of the closed loop system,  $\Delta(s)$  is Hurwitz, the signature of  $\delta(s)$  is as follows and can be easily realized by the Theorem III.1 in the previous section as

$$\sigma(\delta(s, K_i, K_p, K_d)) = n - m + r + 2u \quad (3.14)$$

Therefore the gain stabilization problem has been reduced to a root counting problem for the equation  $\delta(s)$  where it is desired to have  $n + r + u$  roots on the left half of the complex plane and  $m - u$  roots on the right half of the complex plane. In order to analyze the phase movement, substitute  $s = j\omega$  and decompose into real and imaginary parts of  $\delta(j\omega)$  into  $\delta_r(\omega)$  and  $\delta_i(\omega)$  by

$$\begin{aligned} \delta(j\omega) &= \frac{[N_p(j\omega)N_c(j\omega) + e^{-j\theta}D_p(j\omega)D_c(j\omega)]N_p(-j\omega)}{D_p(j\omega)D_p(-j\omega)} \\ &= |H_p(j\omega)|^2 N_c(j\omega) + e^{-j\theta}H_p(-j\omega)D_c(j\omega) \end{aligned} \quad (3.15)$$

Let  $H_p(-j\omega) = H_{pr}(\omega) + jH_{pi}(\omega)$ , where both  $H_{pr}(\omega)$  and  $H_{pi}(\omega)$  become real rational functions. Because we know  $N_c(j\omega)$  and  $D_c(j\omega)$  exactly, then

$$\begin{aligned} \delta(j\omega) &= |H_p(j\omega)|^2 (K_i - K_d\omega^2 + j\omega K_p) + (\cos\theta - j\sin\theta)(H_{pr}(\omega) + jH_{pi}(\omega))(j\omega - T\omega^2) \\ &= \left\{ |H_p(j\omega)|^2 (K_i - K_d\omega^2) + \omega(\sin\theta - T\omega\cos\theta)H_{pr}(\omega) - \omega(\cos\theta + T\omega\sin\theta)H_{pi}(\omega) \right\} \\ &\quad + j\omega \left\{ |H_p(j\omega)|^2 K_p + (\cos\theta + T\omega\sin\theta)H_{pr}(\omega) + (\sin\theta - T\omega\cos\theta)H_{pi}(\omega) \right\} \end{aligned} \quad (3.16)$$

Let new functions  $U(\omega)$  and  $V(\omega)$  represent

$$\begin{aligned} U(\omega) &= (\sin\theta - T\omega\cos\theta) \\ V(\omega) &= (\cos\theta + T\omega\sin\theta) \end{aligned} \quad (3.17)$$

then the above equation can be reduced into

$$\begin{aligned}
\delta(j\omega) &= \left\{ |H_p(j\omega)|^2 (K_i - K_d\omega^2) + \omega(U(\omega)H_{pr}(\omega) - V(\omega)H_{pi}(\omega)) \right\} \\
&\quad + j\omega \left\{ |H_p(j\omega)|^2 K_p + V(\omega)H_{pr}(\omega) + U(\omega)H_{pi}(\omega) \right\} \\
&= \delta_r(j\omega) + j\omega\delta_i(j\omega)
\end{aligned} \tag{3.18}$$

And the real part of characteristic rational function,  $\delta_r(\omega)$  in (3.18), can be restated as of following;

$$\begin{aligned}
\delta_r(j\omega) &= |H_p(j\omega)|^2 (K_i - K_d\omega^2) + \omega(U(\omega)H_{pr}(\omega) - V(\omega)H_{pi}(\omega)) \\
&= |H_p(j\omega)|^2 \begin{bmatrix} -\omega^2 & 1 \\ K_d & K_i \end{bmatrix} + \omega(U(\omega)H_{pr}(\omega) - V(\omega)H_{pi}(\omega))
\end{aligned} \tag{3.19}$$

Let  $l \times 2$  matrix  $A(\omega)$  and  $l$  vector  $b(\omega)$  denote

$$\begin{aligned}
A(\omega) &= |H_p(j\omega)|^2 \begin{bmatrix} -\omega^2 & 1 \end{bmatrix} \\
b(\omega) &= -\omega(U(\omega)H_{pr}(\omega) - V(\omega)H_{pi}(\omega))
\end{aligned} \tag{3.20}$$

By the theorem III.1, we can systemically arrange the series of signs,  $\{i_1, i_2, i_3, \dots, i_{l-1}, i_l\}$  to satisfy the signature condition shown in (3.14) from (3.18) along with linear program arranged by such as (3.24) and (3.25). As shown (3.18), the signature can be calculated from given plant's empirical frequency data only, and then the set of feasible strings are attained by (3.19). Let  $F^*$  denote the set of feasible sign strings,  $F_t$  any possible string set and  $T$  all the possible string sets then,

$$\gamma(F_t) = I_1 \{i_1 - 2i_2 + 2i_3 + \dots + 2(-1)^{l-2}i_{l-1} + (-1)^{l-1}i_l\} + 1 \tag{3.21}$$

where  $I_k = \text{sgn} \left[ \frac{d\delta_i(\omega_k)}{d\omega} \right]$  and  $i_k = \text{sgn}[\delta_r(\omega_k)]$ ,  $k = 1, 2, 3, \dots, l$

$$F^* = \{ t \in T \mid \forall \gamma(F_t) = m - n + r + 2u \} \tag{3.22}$$

The set of controllers in  $[K_i K_p K_d]^T$  is determined for a given plant with rational transfer function if and only if the following conditions hold:

- $F^*$  is not an empty set that is at least one feasible string exist.
- There exist at least one more string  $F_t = \{i_1, i_2, i_3, \dots, i_{l-1}, i_l\} \in F^*$  and values of  $K_i$  and  $K_d$  such that for all  $k = 1, 2, 3, \dots, l$

$$N(-j\omega_k) \neq 0 \text{ and } i_k \cdot \delta_r(\omega) > 0 \quad (3.23)$$

, thus when  $i_k = 1$ ,

$$A_k(\omega) \begin{bmatrix} K_d \\ K_i \end{bmatrix} > b_k(\omega), \text{ for } k = 1, 2, 3, \dots, l \quad (3.24)$$

and when  $i_k = -1$ ,

$$A_k(\omega) \begin{bmatrix} K_d \\ K_i \end{bmatrix} < b_k(\omega), \text{ for } k = 1, 2, 3, \dots, l \quad (3.25)$$

Also if there exist a set of values in  $K_i, K_d$  values for a fixed  $K_p$  is the unions of all  $K_i, K_d$  values satisfying (3.24) or (3.25).

A detailed proof for the above theorem can be found in [2].

Based on previous work, we seek an algorithm which systematically search entire controller set that can be divided into two parts: one is the case that a specific fixed  $K_p$  gain is given and the other is that a finite interest range of  $K_p$  is entered by the user. The inputs are (i) plant data, (ii) desired minimum phase margin and (iii)  $K_p$  value for the first situation or (iii)  $K_p$  range and desired partition in  $K_p$  range for the other. The controller's structure is fixed and given. One can get whole controller sets satisfying performance specifications in an illustrative way with the algorithm as follows:



- Step 1: Input plant data and required minimum phase margin
- Step 2: From given plant data, by (3.18) determine  $\delta_r(\omega)$  and  $\delta_i(\omega)$  with respect to each  $\omega$  frequency.
- Step 3: For various  $K_p$  values, seek every possible number of real roots of  $\delta_i(\omega)$
- Step 4: Get input of a specific desired  $K_p$  value or  $K_p$  range and its partition for 3D image of entire controller sets.
- Step 5: By (3.22) find every possible sign string set utilizing Chapter II, Section E and from (3.24) and (3.25) construct linear programs (LPs) with respect to each sign string. All convex sets from each LPs by each sign string are to be added into the union set.
- Step 6: Verify the result.

Consider the following examples in next section.

#### D. Illustrative Examples

**Example III.1.** This example is based on Example 4.1 of [2]. Assume that we have no exact mathematical plant model but have only frequency data from the plant shown in Figs. 8 and 9. We will carry out the theory and algorithm introduced in this chapter.

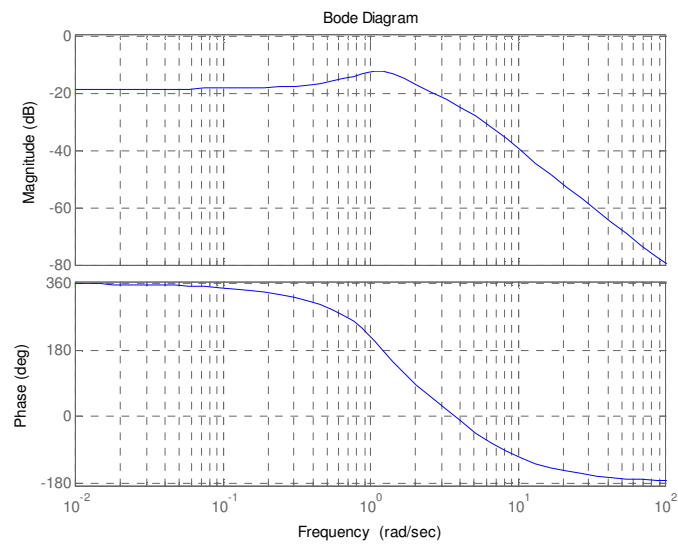


Fig. 8. Bode plot of the plant's frequency response

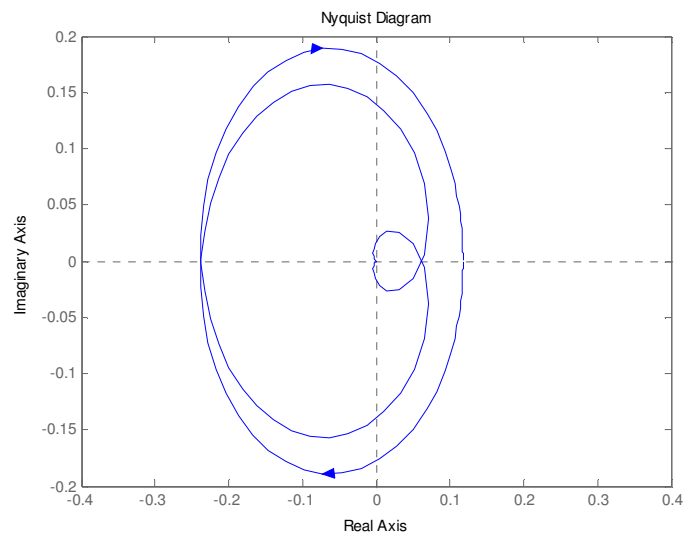


Fig. 9. Nyquist plot of the plant's frequency response

Find the entire PID controller sets to satisfy the phase margin which is more than at least  $30^\circ$ . Select T as  $10^{-4}$ .

The high frequency slope of the Bode magnitude plot is  $-80 - (-40) = -2 \cdot 20\text{db/decade}$  and thus  $n - m = 2$ . The total change of phase is  $-540$  degrees and so

$$-6 \frac{\pi}{2} = -\left\{ (n - m) - 2(r(D_p(s)) - r(N_p(s))) \right\} \frac{\pi}{2} \quad (3.26)$$

And since the plant is stable,  $r(D_p(s)) = 0$ , giving  $r(N_p(s)) = 2$ . By Theorem III.1, the required signature for stability can now be determined as

$$\sigma(\delta(s, K)) = \left( \text{sgn} \left[ \frac{d\delta_i(\omega)}{d\omega} \right]_{\omega=\omega_i} \left\{ i_1 - 2i_2 + 2i_3 \cdots + 2(-1)^{l-1} i_{l-1} + (-1)^l i_l \right\} \frac{1}{2} + 1 \right) = 8 \quad (3.27)$$

where  $i_k (k = 1, 2, 3, \dots, l)$  is the root of  $\delta_i(\omega)$ . It is observed that at least 8 roots in the imaginary part of  $\delta(j\omega)$  are required to yield feasible controller gains. Repeat the rational function  $\delta_r(\omega)$  and  $\delta_i(\omega)$

$$\begin{aligned} \delta_r(\omega) &= |H_p|^2 (K_i - K_d \omega^2) + \omega(U \cdot H_{pr} - V \cdot H_{pi}) \\ \delta_i(\omega) &= |H_p|^2 K_p + V \cdot H_{pr} + U \cdot H_{pi} \\ \delta(\omega) &= \delta_r(\omega) + j\omega\delta_i(\omega) \end{aligned} \quad (3.28)$$

As shown in (3.28), it is obvious that  $K_p$  is independent variable to determine the roots of  $\delta_i(\omega)$ , thus it should be chosen such that  $\delta_i(\omega)$  has more than 7 roots over  $\omega = (-\infty, \infty)$  since there is additional root 0 in the imaginary part. In order to analyze how many roots  $\delta_i(\omega)$  would get, let a new rational function,  $f(\omega)$  denote as

$$f(\omega) = K_p(\omega) = -\frac{V \cdot H_{pr} + U \cdot H_{pi}}{|H_p|^2} \quad (3.29)$$

which is derived from  $0 = |H_p|^2 K_p + V \cdot H_{pr} + U \cdot H_{pi}$

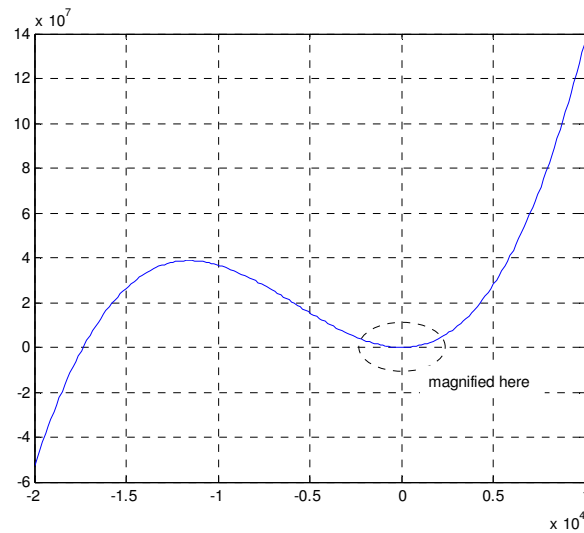


Fig. 10. Plot of  $f(\omega)$  with respect to the frequency

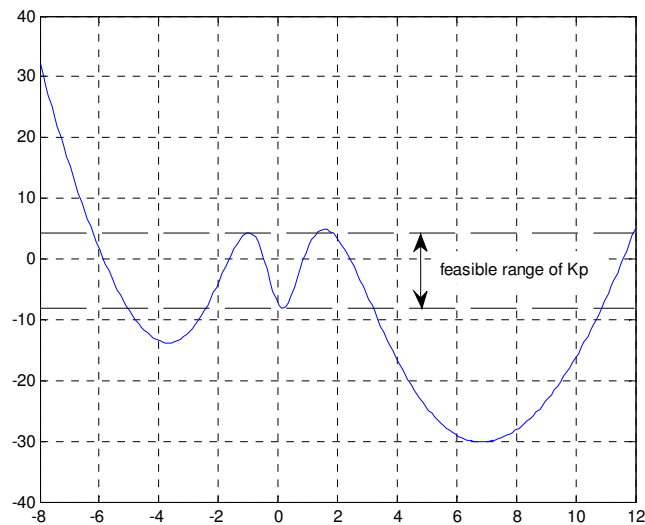


Fig. 11. Magnification of Fig. 10

As shown in Figs. 10 and 11 of  $f(\omega)$ ,  $K_p$  should be determined  $(-8.1218, 4.2871)$ .

Choose  $K_p$  as 3, then the real roots of  $\delta_i(\omega)$  shown in Fig. 12 can be found as

$$\omega_k = (-17348, -6.1137, -1.3051, -0.6905, 0, 1.1206, 2.0628, 11.839) \quad (3.30)$$

, which is leading to the string set as  $i_1 - 2i_2 + 2i_3 - 2i_4 + 2i_5 - 2i_6 + 2i_7 - i_8 = 14$ . This permits only one feasible set  $F^*$  of

$$F^* = \{ i_1, i_2, i_3, i_4, i_5, i_6, i_7, i_8 \} = \{ 1, -1, 1, -1, 1, -1, 1, -1 \} \quad (3.31)$$

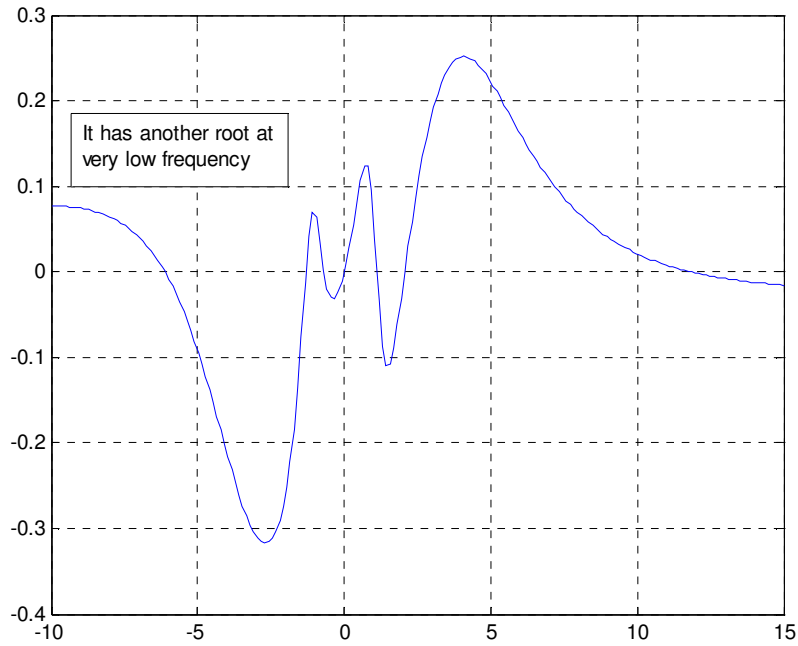


Fig. 12.  $\delta_i(\omega)$  plot to examine its real roots

Thus, we have the following linear programming for the performance of phase margin

30°:

$$-3.3227 \cdot 10^{-7} K_d + 1.104 \cdot 10^{-15} K_i > -0.011542$$

$$-2.9408 K_d + 0.078678 K_i < 17.088$$

$$-8.8664 K_d + 5.2056 K_i > -21.708$$

$$-1.5719 K_d + 3.2968 K_i < 10.514$$

$$K_i > 0$$

$$\begin{aligned}
 -7.2052 K_d + 5.738 K_i &< 18.666 \\
 -7.4487 K_d + 1.7505 K_i &> -25.05 \\
 -0.77056 K_d + 0.0054975 K_i &< 8.776
 \end{aligned}
 \tag{3.32}$$

Fig. 13 shows the complete gain sets of PID controller for  $K_p = 3$ , which is the union set satisfying every constraints shown in (3.32).

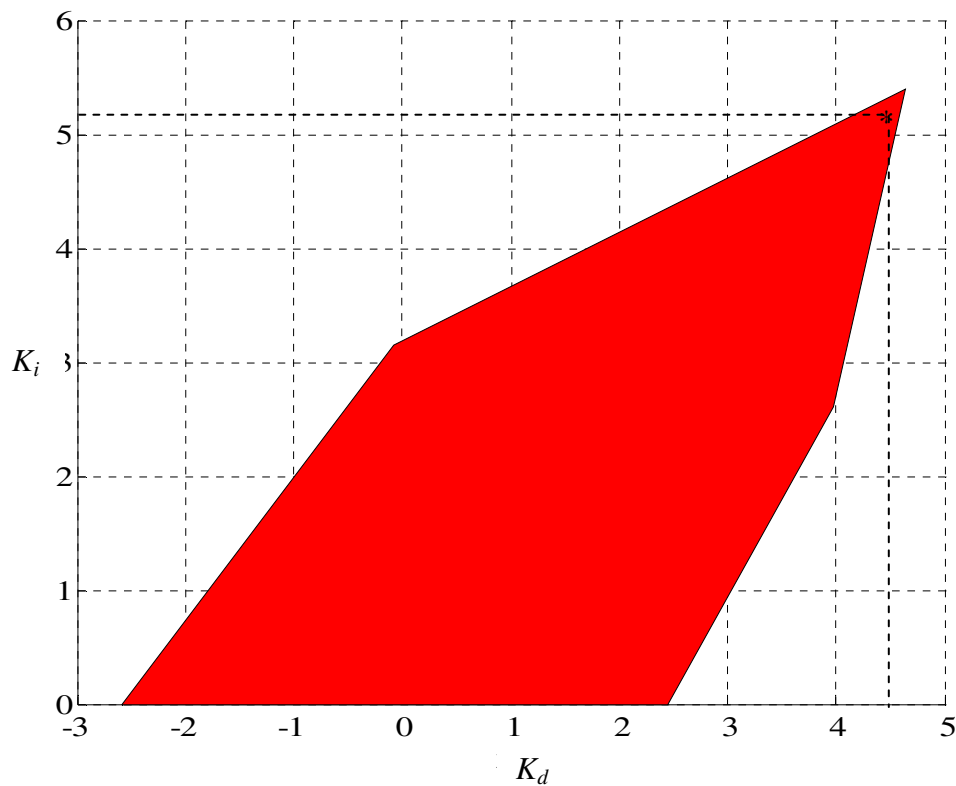


Fig. 13. Entire  $K_d, K_i$  controller set satisfying  $PM > 30^\circ$

The tested point is specified as \* in Fig. 13, which makes a verification whether it satisfies the control system's performance specification – phase margin in Fig. 14.

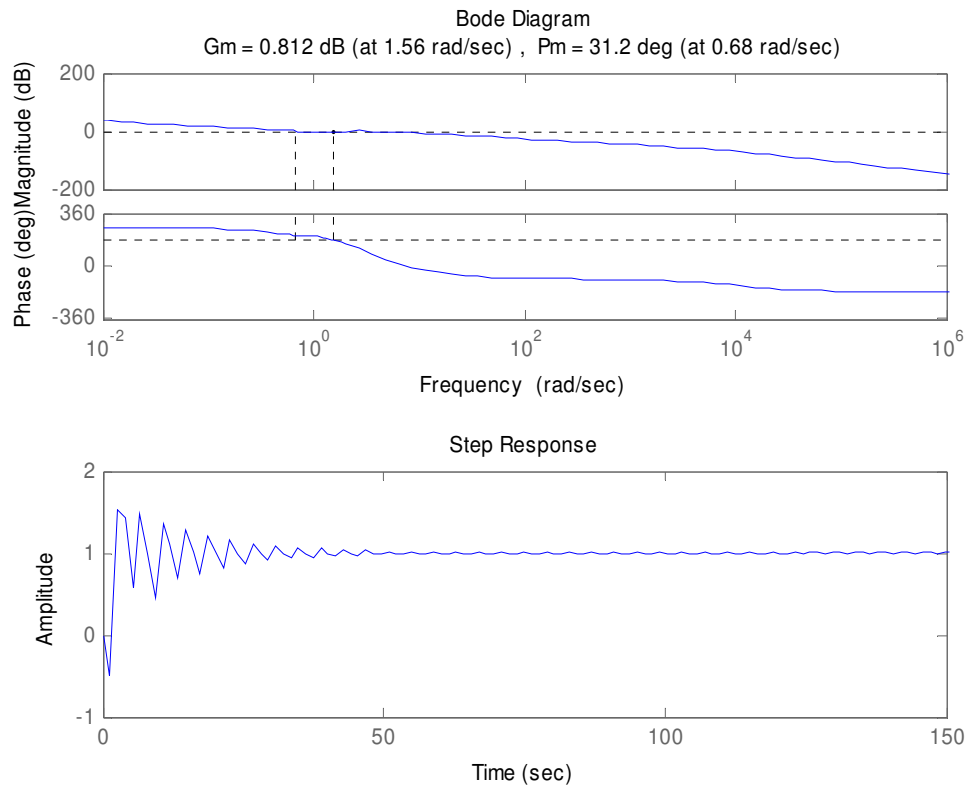


Fig. 14. Bode diagram and step response of the system by the selected controller

By sweeping over  $K_p$  range which ensures the feasible controller gain set, here  $(-8.1218, 4.2871)$ , we determine the entire set of PID gains to guarantee the given phase margin shown in Fig. 15.

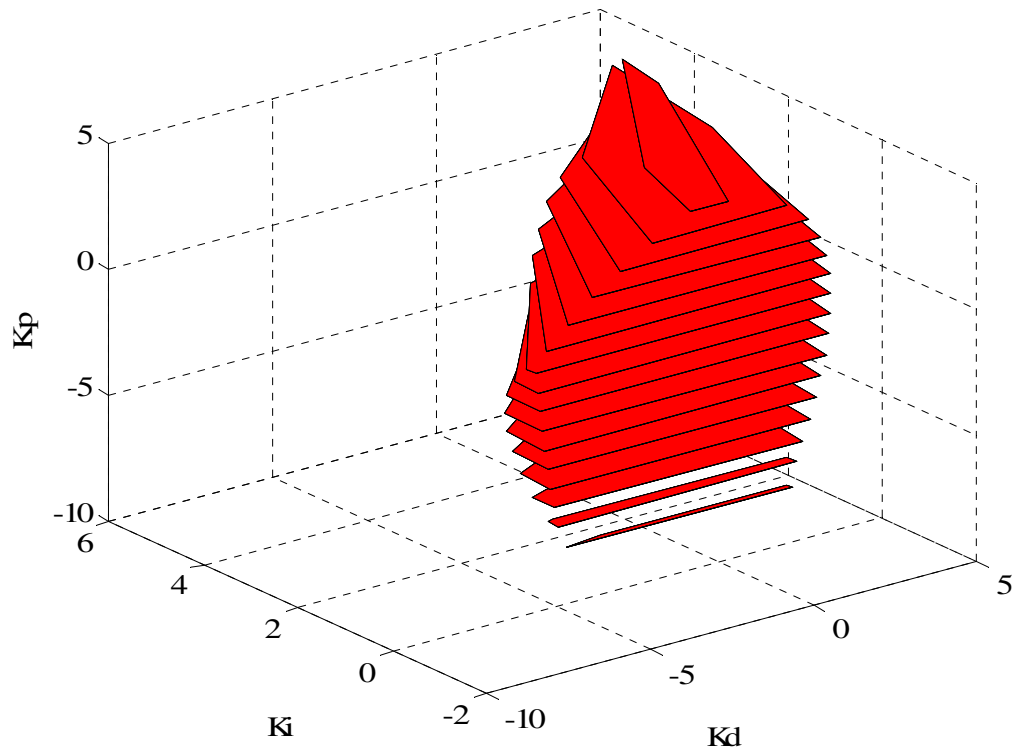


Fig. 15. Entire PID controller set for Example III.1

One can wonder this is stabilizing set or just satisfying phase margin. In order to guarantee both criteria, we need to intersect two subsets each other. This is shown in the next example III.2.

**Example III.2.** Consider the same plant in Example III.1. At this example, choose  $K_p = 4.2$ . Then, the real roots of  $\delta_i(\omega)$  can be found as

$$\omega_k = (-17348, -6.2084, -1.0571, -0.8985, 0, 1.2918, 1.8508, 11.935) \quad (3.33)$$



which is leading to the string set as  $i_1 - 2i_2 + 2i_3 - 2i_4 + 2i_5 - 2i_6 + 2i_7 - i_8 = 14$ . This is also permits only one feasible set  $F^*$  of

$$F^* = \{ i_1, i_2, i_3, i_4, i_5, i_6, i_7, i_8 \} = \{ 1, -1, 1, -1, 1, -1, 1, -1 \} \quad (3.34)$$

Thus, we have the following linear programming for the performance of phase margin  $30^\circ$ :

$$\begin{aligned} -3.3227 \cdot 10^{-7} K_d + 1.104 \cdot 10^{-15} K_i &> -0.011542 \\ -2.8617 K_d + 0.074245 K_i &< 16.806 \\ -6.2929 K_d + 5.6317 K_i &> -2.034 \\ -3.8597 K_d + 4.7811 K_i &< 7.7747 \\ K_i &> 0 \\ -8.8035 K_d + 5.2756 K_i &< 7.815 \\ -8.0129 K_d + 2.3391 K_i &> -21.695 \\ -0.75761 K_d + 0.0053189 K_i &< 8.7 \end{aligned} \quad (3.35)$$

From (3.32) we have red and blue area for the given  $30^\circ$  phase margin. In Fig. 16, the yellow region represents the stability area, i.e. when phase margin  $\varphi$  is set to 0. We can achieve both phase margin and stability in the blue area that two regions intersect. Fig. 16 illustrates the result of this example.

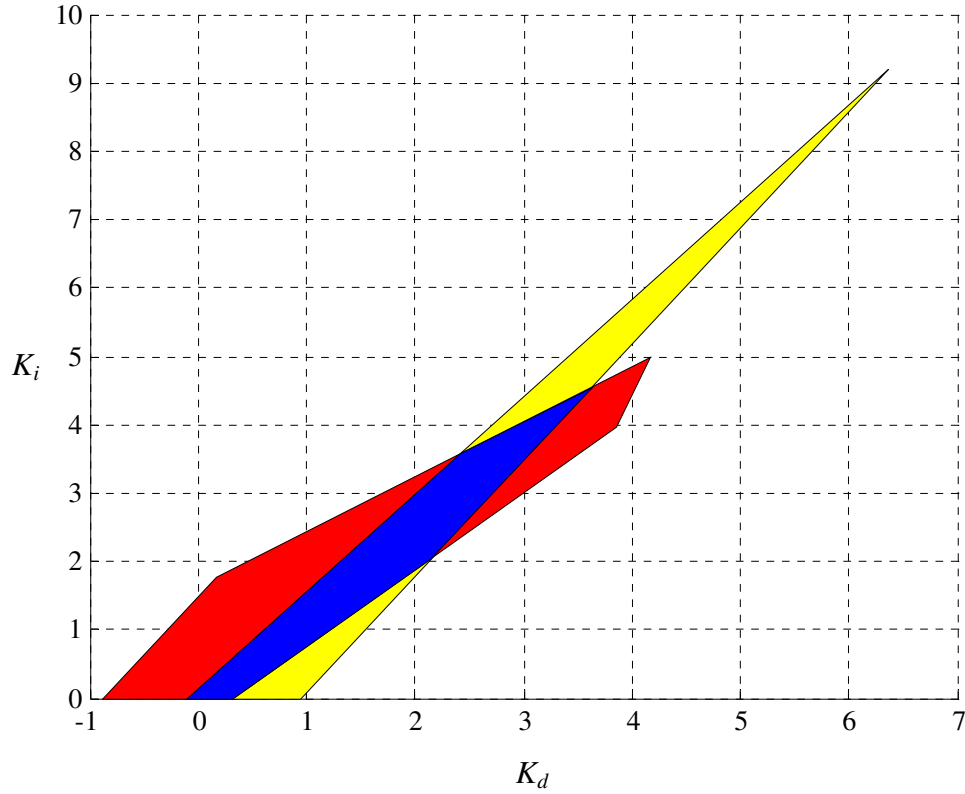


Fig. 16. Stabilizing and performance subset

**Example III.3.** From the given exact plant, show the entire controller gain set for satisfying minimum phase margin respect to various numbers of phase margin. Consider the plant  $H_p(s)$

$$H_p(s) = \frac{1}{s^3 + 6s^2 + 5s} \quad (3.36)$$

Set  $K_p$  range as  $(0, 80)$  and get the  $K_d, K_i$  phase margin subset respect to each discrete 10 number of  $K_p$  ( $K_p = 0, 8.89, 17.78, 26.67, 35.56, 44.44, 53.33, 62.22, 71.11, 80$ ).

By Theorem III.1,

$$2(n - m + r + 2u - 1) = 2(3 + 2 + 0 - 1) = 8 \quad (3.37)$$

$$\text{sgn}[\dot{\delta}_i(\omega)](i_1 - 2i_2 + 2i_3 \cdots + 2(-1)^{l-2}i_{l-1} + (-1)^{l-1}i_l) = 8 \quad (3.38)$$

It is obvious that we need at least 5 real roots of  $\omega\delta_i(\omega)$  to secure at least one set of feasible controller gain set. It is noted that the admissible  $K_p$  range makes a change respect to various phase margin condition referring to Fig. 17. For instance when phase margin is given by  $45^\circ$ , the acceptable  $K_p$  spans from 0 to 37.37. It is concluded that smaller phase margin is, smaller the gain set becomes and it is shown in Figs. 18, 19, 20.

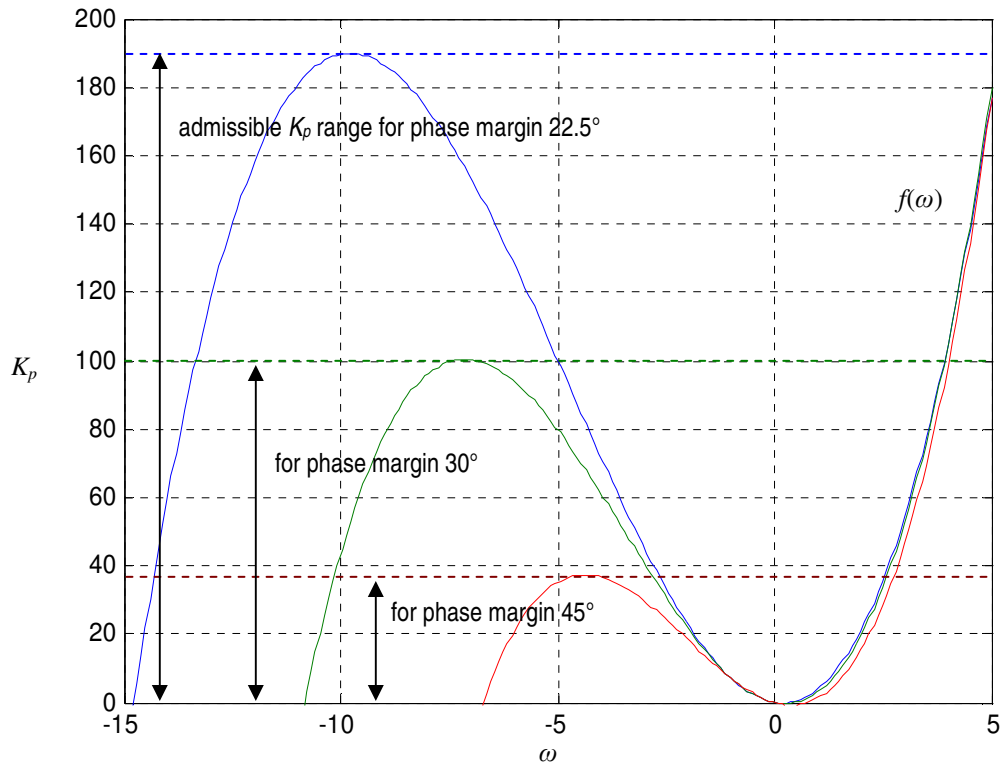


Fig. 17.  $f(\omega)$  plot for determining admissible  $K_p$  range

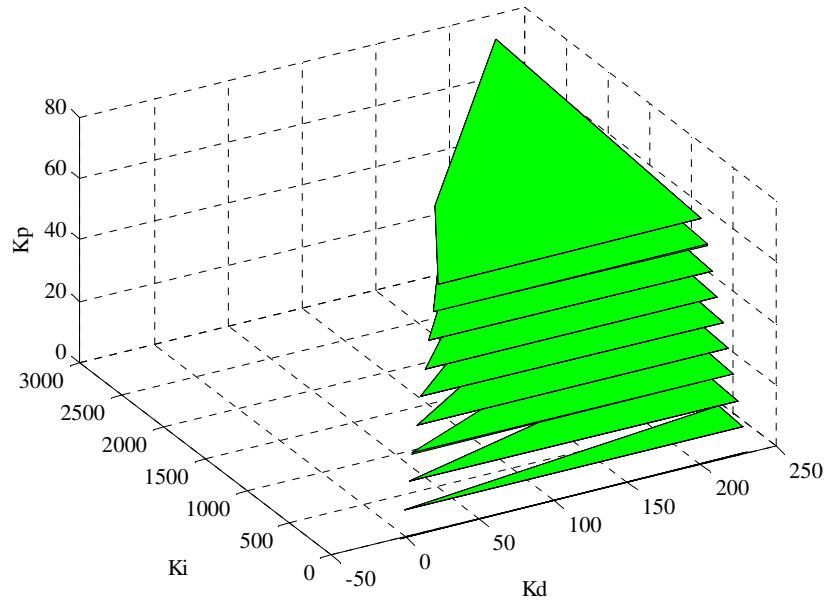


Fig. 18. Entire PID controller sets for  $PM = 22.5^\circ$

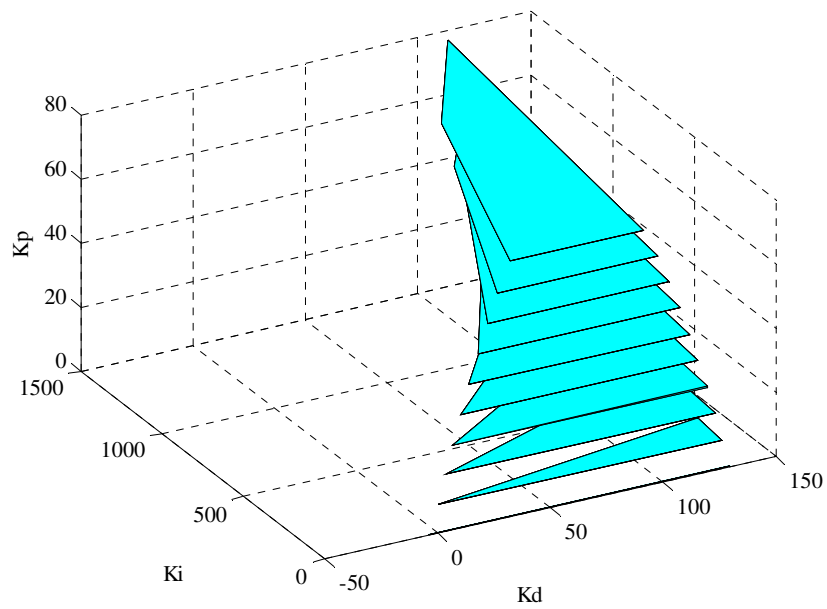


Fig. 19. Entire PID controller sets for  $PM = 30^\circ$

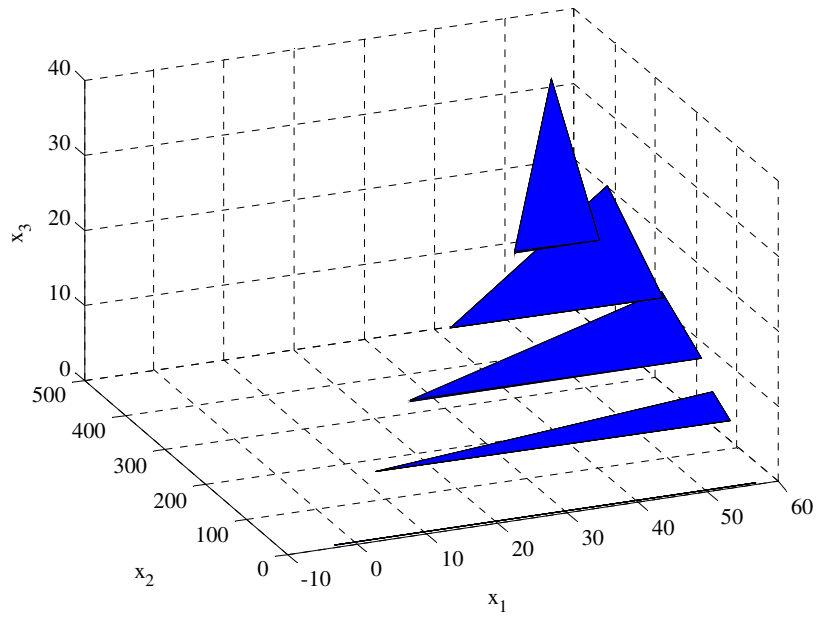


Fig. 20. Entire PID controller sets for  $PM = 45^\circ$

## CHAPTER IV

FIXED STRUCTURE CONTROLLER SYNTHESIS FOR  
 $H_\infty$  NORM CONSTRAINT

## A. Introduction

$H_\infty$  control theory was extensively studied by Doyle, Glover *et. al.* [10] for robust stability and performance control in 1980's. It was developed originally by Zames(1981), although an earlier use of  $H_\infty$  optimization in an engineering context can be found in Helton(1976). In [11] the standard  $H_\infty$  optimal control problem is well described as to find all stabilizing controllers  $K$  which minimize

$$\|F_l(P, K)\|_\infty = \max_{\omega} \overline{\sigma}(F_l(P, K)(j\omega)) \quad (4.1)$$

Ho [12] criticized the existing mature  $H_\infty$  control method by its inevitable higher order controller being comparable to that of the plant as well as the intense computational burden and its intractability or conservatism to get only limited controller sets. In [13] Tantaridis *et. al.* also pointed out same side effect of the Youla-Jabr-Bongiorno-Kucera(YJBK) characterization of all stabilizing controllers for a given plant. By noting that most of industry controllers are either PI(or PID) or simple first-order lead/lag compensators, Ho [12] proposed a fixed structured PID controller synthesis method which is a systematic way to seize entire controller gain sets. Borrowing the main  $H_\infty$  idea, he developed a parametric approach to take advantage of nowadays' highly developed computers. We would like to proceed with our discussion over the

determining controller from the plant's frequency response without knowing the transfer function itself. However, in [12] we can not find the equation for the frequency response, instead we continue the decomposition of  $K_p$  gain against  $K_i$  and  $K_d$  gains in this chapter following which is similar to that of Chapter III. Indeed, the example result in the later part of this chapter shows the coincidence with that of [12], for we are using the same literature with it.

## B. Background Theory

We need to start first with the following lemma, which will be modified relevantly with this research such as the previous Chapter.

**Lemma IV.1** [14]. Let  $F(s) = \frac{N_F(s)}{D_F(s)}$  be a stable and proper rational function, where

$N_F(s)$  and  $D_F(s)$  are polynomials with  $\deg[D_F(s)] = \alpha$ . Then  $\|F(s)\|_\infty < 1$  if and only if

$$(1) |n_\alpha| < |d_\alpha|;$$

$$(2) D_F(s) + e^{j\theta}N_F(s) \text{ is Hurwitz for all } \theta \text{ in } [0, 2\pi),$$

where  $n_\alpha$  and  $d_\alpha$  are the leading coefficients of  $N_F(s)$  and  $D_F(s)$ , respectively.

Let the weighting function  $W(s) = W_n(s)/W_d(s)$ , where  $W_n(s)$  and  $W_d(s)$  are coprime polynomials; moreover,  $W_d(s)$  is Hurwitz [12].

In [15], various performance specifications could be made by using the  $H_\infty$  norm of weighted versions of the transfer functions like the one shown in (4.2). This is leading Lemma IV.1 to Lemma IV.2 as of following.

**Lemma IV.2** Consider the same transfer function  $H_p(s)$  and PID controller  $C(s)$  in section B, Chapter III. The sensitivity function  $S(s)$  of  $H_p(s)$  is expressed by

$$S(s) = \frac{1}{(1 + C(s)H_p(s))} = \frac{D_c(s)D_p(s)}{D_c(s)D_p(s) + N_c(s)N_p(s)} \quad (4.2)$$

Then  $\|W(s)S(s)\|_\infty < \gamma$  if and only if the revised closed loop characteristic equation  $\Delta(s)$ ,  $\Delta(s) = W_n(s)D_c(s)D_p(s) + \gamma e^{-j\theta}W_d(s) [N_c(s)N_p(s) + D_c(s)D_p(s)]$ , is Hurwitz for all  $\theta$  in  $[0, 2\pi)$ .

**Lemma IV.3.** Consider the same transfer function  $H_p(s)$  and PID controller  $C(s)$  in Lemma IV.2. The complementary sensitivity function  $T(s)$  of  $S(s)$  is expressed by

$$T(s) = \frac{N_c(s)N_p(s)}{D_c(s)D_p(s) + N_c(s)N_p(s)} \quad (4.3)$$

Then  $\|W(s)T(s)\|_\infty < \gamma$  if and only if the revised closed loop characteristic equation  $\Delta(s)$ ,  $\Delta(s) = W_n(s)N_c(s)N_p(s) + \gamma e^{-j\theta}W_d(s) [N_c(s)N_p(s) + D_c(s)D_p(s)]$ , is Hurwitz for all  $\theta$  in  $[0, 2\pi)$ .

For the sensitivity function  $H_\infty$  constraint specification can be achieved by same manner of the complementary sensitivity case, we take a close examine of Lemma IV.3 and employ it to set the position casting synthesis  $H_\infty$  PID controllers into the simultaneous polynomial stabilizing problem.



### C. Expansion of Characteristic Equation for PID Controllers and Algorithm

In this section, regarding to Lemma IV.3, we now expand the modified characteristic equation in the same manner appeared in Chapter III in order to make use of the generalized Hermite-Biehler theorem only for using empirical data.

Reconsider the complex characteristic polynomial given in Lemma IV.3.

$$\Delta(s) = W_n(s)N_c(s)N_p(s) + \gamma e^{-j\theta} W_d(s) [N_c(s)N_p(s) + D_c(s)D_p(s)] \quad (4.4)$$

Now we need to reorganize a new rational complex function  $\delta(s)$  as  $\delta(j\omega) = \delta_r(\omega) + j\delta_i(\omega)$  to utilize the plant's empirical data in terms of frequency response and interlacing property from the decomposition of the characteristic function.

$$\text{Let } H_p(-j\omega) = H_{pr}(\omega) + jH_{pi}(\omega)$$

$$\delta(j\omega) = N_c(W_n + \gamma e^{-j\theta} W_d) |H_p(j\omega)|^2 + \gamma(\cos\theta - j\sin\theta)W_d(j\omega - T\omega^2)(H_{pr} + jH_{pi}) \quad (4.5)$$

$$\text{Define } U(\omega) = \sin\theta - T\omega\cos\theta,$$

$$V(\omega) = \cos\theta + T\omega\sin\theta,$$

$$L_r(\omega) + jL_i(\omega) = W_n(j\omega) + \gamma e^{-j\theta} W_d(j\omega),$$

$$M_r(\omega) + jM_i(\omega) = \gamma W_d(j\omega) (U(\omega) + jV(\omega))(L_r(\omega) - jL_i(\omega)) \quad (4.6)$$

Moreover,  $\delta(j\omega)$  needs additional multiplier  $(L_r - jL_i)$  for the division of PID controller set,  $\mathbf{K} = [K_d \ K_p \ K_i]^T$ . Let denote this new rational function as  $\delta^*(j\omega)$ , then

$$\begin{aligned} \delta^*(j\omega) &= \delta(j\omega) (L_r - jL_i) \\ &= (K_d + jK_p\omega - K_i\omega^2)(L_r^2 + L_i^2)|H_p|^2 + \gamma\omega W_d(U + jV) (L_r - jL_i)(H_{pr} + jH_{pi}) \\ &= \{(K_d - K_i\omega^2) (L_r^2 + L_i^2)|H_p|^2 + \omega(M_r H_{pr} - M_i H_{pi})\} \\ &\quad + j\omega\{K_p(L_r^2 + L_i^2)|H_p|^2 + M_r H_{pi} + M_i H_{pr}\} \\ &= \delta_r^*(\omega) + j\omega\delta_i^*(\omega) \end{aligned} \quad (4.7)$$

And the real part of characteristic rational function,  $\delta_r^*(\omega)$  in (4.7), can be restated as of following;

$$\begin{aligned}\delta_r^*(\omega) &= \{(K_d - K_i\omega^2)(L_r^2 + L_i^2)|H_p|^2 + \omega(M_r H_{pr} - M_i H_{pi})\} \\ &= (L_r^2 + L_i^2)|H_p|^2 \begin{bmatrix} -\omega^2 & 1 \end{bmatrix} \begin{bmatrix} K_d \\ K_i \end{bmatrix} + \omega(M_r H_{pr} - M_i H_{pi})\end{aligned}\quad (4.8)$$

Let  $l \times 2$  matrix,  $A(\omega)$  and  $l$  vector,  $b(\omega)$  denote

$$\begin{aligned}A(\omega) &= (L_r^2 + L_i^2)|H_p|^2 \begin{bmatrix} -\omega^2 & 1 \end{bmatrix} \\ b(\omega) &= \omega(M_r H_{pr} - M_i H_{pi})\end{aligned}\quad (4.9)$$

Again, we can systemically arrange the series of signs for  $i_1, i_2, i_3, \dots, i_{l-1}, i_l$  to satisfy the signature condition like Chapter III. The signature can be calculated given plant's empirical frequency data as shown earlier, then the set of feasible strings are attained and let  $F^*$  denote the set of feasible strings, then

$$F^* = \{ t \in T \mid \forall \gamma(F_t) = m - n + r + 2u \} \quad (3.22)$$

The set of controllers in  $[K_i \ K_p \ K_d]^T$  is determined for a given plant with rational transfer function if and only if the following conditions hold:

- $F^*$  is not an empty set that is at least one feasible string exist.
- There exist at least one more string  $F_t = \{i_1, i_2, i_3, \dots, i_{l-1}, i_l\} \in F^*$  and values of  $K_i$  and  $K_d$  such that for all  $k = 1, 2, 3, \dots, l$

$$N(-j\omega_k) \neq 0 \text{ and } i_k \cdot \delta_r(\omega) > 0 \quad (3.23)$$

Also if there exist a set of values in  $K_i, K_d$  values for a fixed  $K_p$  is the unions of all  $K_i, K_d$  values satisfying  $i_k \cdot \delta_r(\omega) > 0$ .

Likewise, linear programming is also organized by (4.9) as

when  $i_k = 1$ ,

$$A_k(\omega) \begin{bmatrix} K_d \\ K_i \end{bmatrix} > b_k(\omega), \text{ for } k = 1, 2, 3, \dots, l \quad (4.10)$$

and when  $i_k = -1$ ,

$$A_k(\omega) \begin{bmatrix} K_d \\ K_i \end{bmatrix} < b_k(\omega), \text{ for } k = 1, 2, 3, \dots, l \quad (4.11)$$

The algorithm which systematically search entire controller set is very similar to the one shown in Chapter III. We can specify a fixed  $K_p$  gain or a finite interest range of  $K_p$  for this objective. The inputs are (i) plant data, (ii) desired  $H_\infty$  constraint and (iii)  $K_p$  value or (iii)  $K_p$  range and desired partition in  $K_p$  range for the other. The controller's structure and the weight function are fixed and given. One can get whole controller sets satisfying performance specifications in an illustrative way with the algorithm as follows:

- Step 1: Input plant data and required minimum  $H_\infty$  constraint
- Step 2: From given plant data, by (4.7) determine  $\delta_r^*(\omega)$  and  $\delta_i^*(\omega)$  with respect to each  $\omega$  frequency.
- Step 3: For various  $K_p$  values, seek every possible number of real roots of  $\delta_i^*(\omega)$
- Step 4: Get input of a specific desired  $K_p$  value or  $K_p$  range and its partition for 3D image of entire controller sets. Set  $\theta$  as a particular value.
- Step 5: By (3.22) find every possible sign string set utilizing Chapter II, Section E and from (4.10) and (4.11) construct linear programs (LPs) with respect to

each sign string. All convex sets from each LPs by each sign string are to be added into the union set,  $P^*$ .

- Step 6: Varying  $\theta$  from 0 until  $2\pi(-)$  and repeat step 4, and 5. At each loop, alternate  $\theta$  and intersect the convex set with the result set,  $P = P \cap P^*$
- Step 7: Verify the result  $P$ .

Consider the following examples in next section.

#### D. Illustrative Examples

**Example IV.1.** Consider the plant frequency data in Figs. 21 and 22. Find the entire PID controller sets to satisfy the  $H_\infty$  constraint which is less than 2. Set T is  $10^{-4}$  in the controller and the weight function  $W(s)$  is 1.

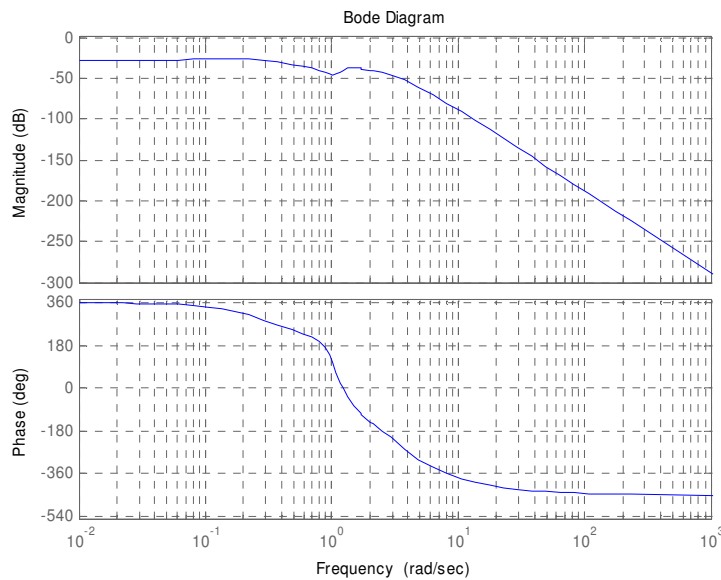


Fig. 21. Bode plot of the Example IV.1 plant

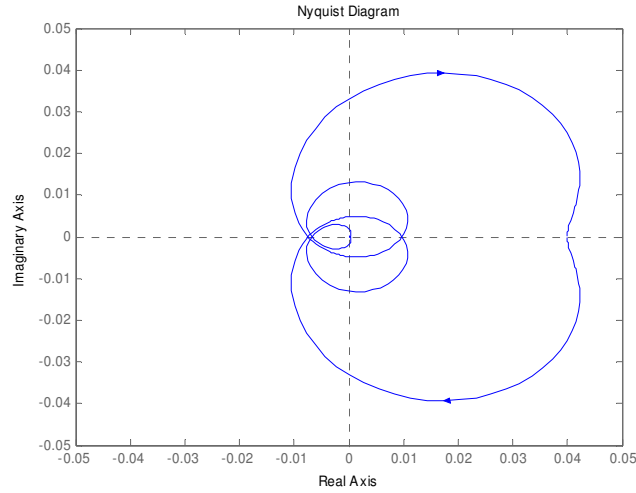


Fig. 22. Nyquist plot of the Example IV.1 plant

The high frequency slope of the Bode magnitude plot is  $-280 - (-180) = -5 \cdot 20\text{db/decade}$  and thus  $n - m = 5$ . The total change of phase is  $-810^\circ$  and so

$$-9\frac{\pi}{2} = -\{(n - m) - 2(r(D_p(s)) - r(N_p(s)))\}\frac{\pi}{2} \quad (4.12)$$

And since the plant is stable,  $r(D_p(s)) = 0$ , giving  $r(N_p(s)) = 2$ . By Theorem III.1, the required signature for stability can now be determined as

$$\sigma(\delta^*(s, K)) = \left( \text{sgn} \left[ \frac{d\delta_i^*(\omega_1)}{d\omega} \right] \left\{ i_1 - 2i_2 + 2i_3 \cdots + 2(-1)^{l-1}i_{l-1} + (-1)^l i_l \right\} \frac{1}{2} + 1 \right) = 11 \quad (4.13)$$

where  $i_k (k = 1, 2, 3, \dots, l)$  is the root of  $\delta_i(\omega)$ . It is observed that at least 11 roots in the imaginary part of  $\delta^*(j\omega)$  are required to yield feasible controller gains. Repeat the rational function  $\delta_r^*(\omega)$  and  $\delta_i^*(\omega)$

$$\delta_r^*(\omega) = (L_r^2 + L_i^2) |H_p|^2 \begin{bmatrix} -\omega^2 & 1 \end{bmatrix} \begin{bmatrix} K_d \\ K_i \end{bmatrix} + \omega (M_r H_{pr} - M_i H_{pi}) \quad (4.14)$$

$$\delta_i^*(\omega) = K_p(L_r^2 + L_i^2)|H_p|^2 + M_r H_{pi} + M_i H_{pr} \quad (4.15)$$

It should be chosen such that  $\delta_i^*(\omega)$  has more than 10 roots over  $\omega = (-\infty, \infty)$  since there is inherent root 0 in the imaginary part. In order to analyze how many roots  $\delta_i^*(\omega)$  would get, let a new rational function,  $f(\omega)$  denote as

$$f(\omega) = K_p(\omega) = -\frac{M_r H_{pi} + M_i H_{pr}}{(L_r^2 + L_i^2)|H_p|^2} \quad (4.16)$$

$f(\omega)$  is illustrated in Fig. 23 to show admissible  $K_p$  range taken by 12 discrete  $\theta$  value as ( 0, 32.722°, 65.444°, 98.166°, 130.89°, 163.61°, 196.33°, 229.05°, 261.78°, 294.5°, 327.22°, 359.9° ).

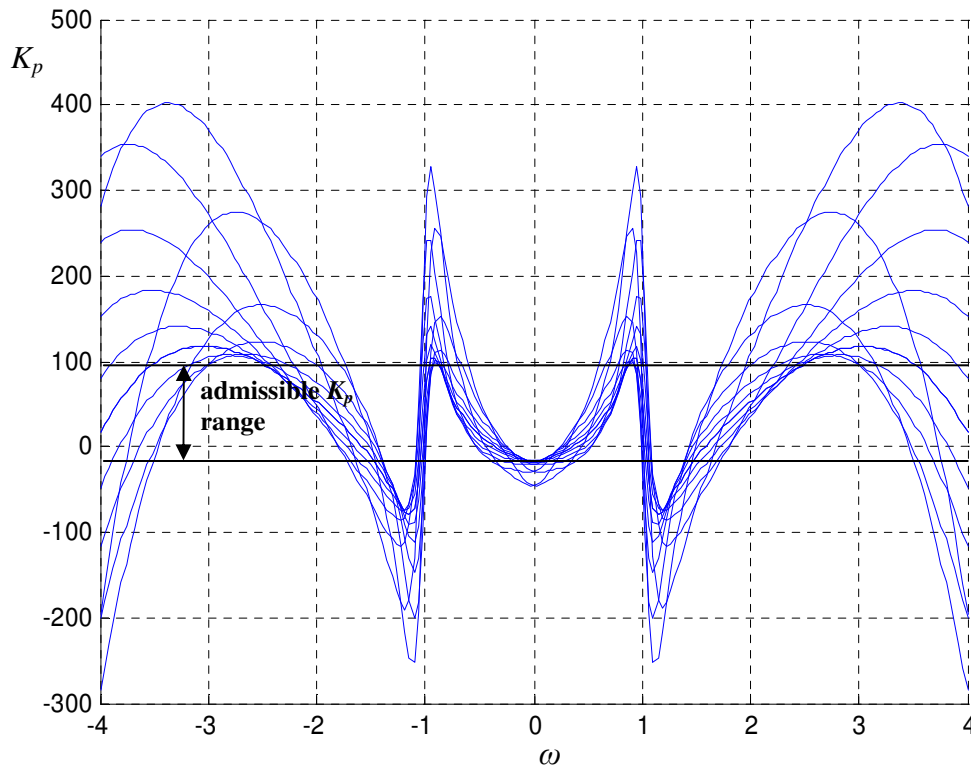


Fig. 23.  $f(\omega)$  plot for the admissible  $K_p$  range about  $\theta = [0, 2\pi)$

When  $\theta = 0$ , by (4.15) we obtain the real roots of  $\delta_i^*(\omega)$  as of followings:

$$\begin{aligned} \omega_i = & -360.63, -3.7217, -2.1734, -0.99172, -0.79533, \\ & 0, 0.79533, 0.99172, 2.1734, 3.7217, 360.63 \end{aligned} \quad (4.17)$$

$$\operatorname{sgn} \left[ \frac{d\delta_i^*(\omega)}{d\omega} \right]_{\omega=\omega_i} = -1 \quad (4.18)$$

(4.17) and (4.18) lead to determining string set by

$$-1 \cdot \{i_1 - 2i_2 + 2i_3 - 2i_4 + 2i_5 - 2i_6 + 2i_7 - 2i_8 + 2i_9 - 2i_{10} + i_{11}\} = 20 \quad (4.19)$$

which permits only one feasible set  $F^*$  of

$$\begin{aligned} F^* &= \{ i_1, i_2, i_3, i_4, i_5, i_6, i_7, i_8, i_9, i_{10}, i_{11} \} \\ &= \{ -1, 1, -1, 1, -1, 1, -1, 1, -1, 1, -1 \} \end{aligned} \quad (4.20)$$

Then, by (4.20), (4.6) and (4.14) we construct Linear programs (4.10) and (4.11):

$$\begin{aligned} -5.0324e-015 K_d + 3.8694e-020 K_i &< 1.4197e-005 \\ -8.4017 K_d + 0.60656 K_i &> -557.76 \\ -31.375 K_d + 6.6418 K_i &< 483.63 \\ -2.0139 K_d + 2.0476 K_i &> -245.66 \\ -4.79 K_d + 7.5725 K_i &< 117.75 \\ 144 K_i &> 0 \\ -4.79 K_d + 7.5725 K_i &< 117.75 \\ -2.0139 K_d + 2.0476 K_i &> -245.66 \\ -31.375 K_d + 6.6418 K_i &< 483.63 \\ -8.4017 K_d + 0.60656 K_i &> -557.76 \\ -5.0324e-015 K_d + 3.8694e-020 K_i &< 1.4197e-005 \end{aligned} \quad (4.18)$$

From section C, the admissible gain set exist if and only if the following conditions stand:

1.  $v(s) = N_c(s)N_p(s) + D_c(s)D_p(s)$  is Hurwitz;

2.  $\Delta(s) = W_n(s)N_c(s)N_p(s) + \gamma e^{-j\theta}W_d(s) [N_c(s)N_p(s) + D_c(s)D_p(s)]$

is Hurwitz for all  $\theta \in [0, 2\pi)$ ;

3.  $|W(\infty)T(\infty)| = |n_c/d_d| = 0 < 1$ , for the order of  $T(s)$ 's denominator is always

higher than  $T(s)$ 's numerator when the plant is strictly proper function ( $n-m=5$ ).

In this example, increase  $\theta$  value and repeat the same procedure to get similar LPs like (4.18). Iteration is carried out for every discrete  $\theta = 0, 32.722^\circ, 65.444^\circ, 98.166^\circ, 130.89^\circ, 163.61^\circ, 196.33^\circ, 229.05^\circ, 261.78^\circ, 294.5^\circ, 327.22^\circ, 359.9^\circ$ . After intersecting every obtained convex controller set from the iteration, we finally come into the entire controller gain set which contents

$$\left\| W(s) \frac{N_c(s)N_p(s)}{D_c(s)D_p(s) + N_c(s)N_p(s)} \right\|_\infty < \gamma = 2 \quad (4.19)$$

where  $W(s) = 1$  in this example. In Fig. 24, the iterated sets and intersection are shown fixing  $K_p = 70$ .



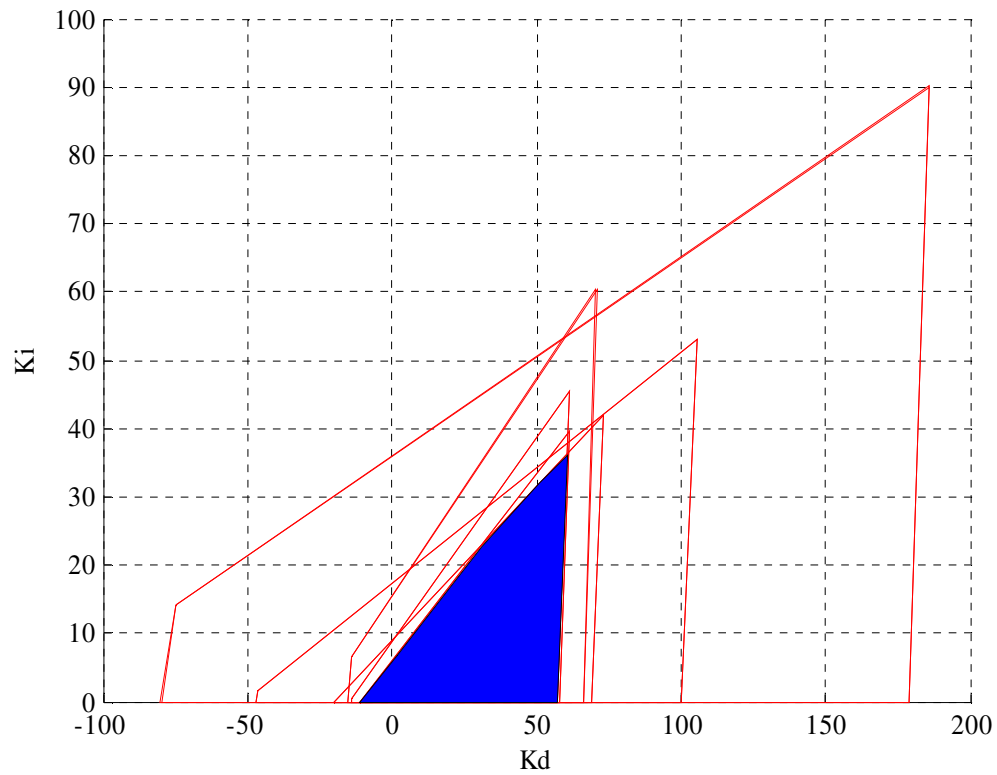


Fig. 24.  $K_d, K_i$  gain set for 12 discrete  $\theta$  values in  $[0, 2\pi)$  and their intersect area in blue

Fig. 25 explains that nominal stability controller set in red becomes smaller to  $H_\infty$  robust PID controller set, which means more conservative design. Not to mention, the blue area in Fig. 25 is identical to the one in Fig. 24.

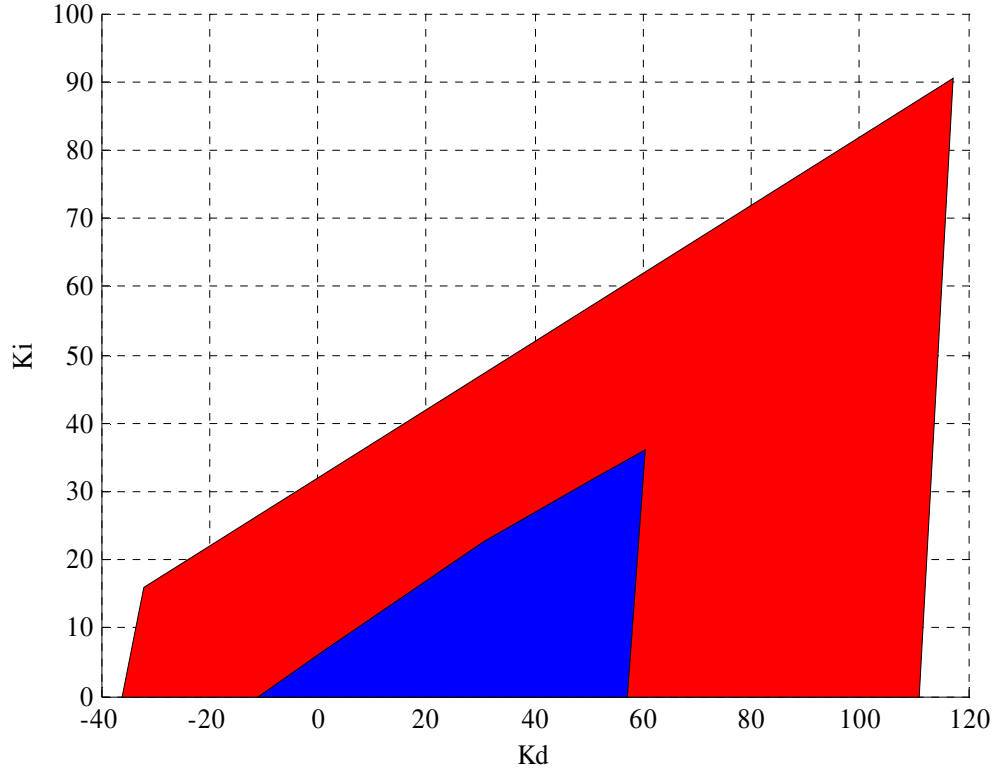


Fig. 25.  $K_d, K_i$  gain set for  $H_\infty$  constraint,  $\gamma = 2$ , when  $K_p = 70$

**Example IV.2.** Reconsider the example in [12] and assume we have only frequency empirical data of the plant shown in Figs. 26 and 27. As [12], we determine the admissible PID controller gain values for which  $\|W(s)T(s)\|_\infty < \gamma = 1$ , where  $T(s)$  is the complementary sensitivity function. Later the result when  $\gamma = 2$  is also shown for the comparison. The weight function  $W(s)$  is chosen as a high pass transfer function:

$$W(s) = \frac{s+0.1}{s+1} \quad (4.20)$$

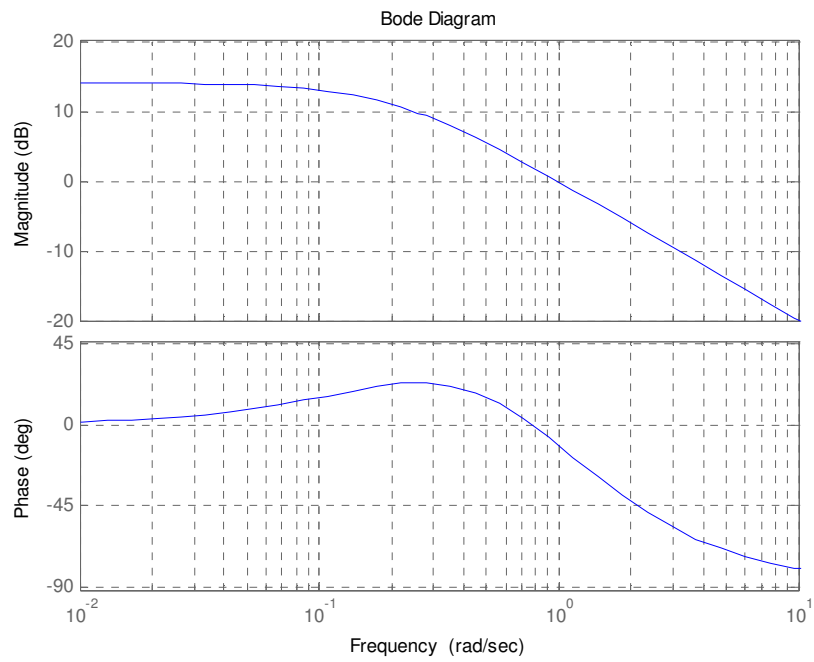


Fig. 26. Bode plot of the plant

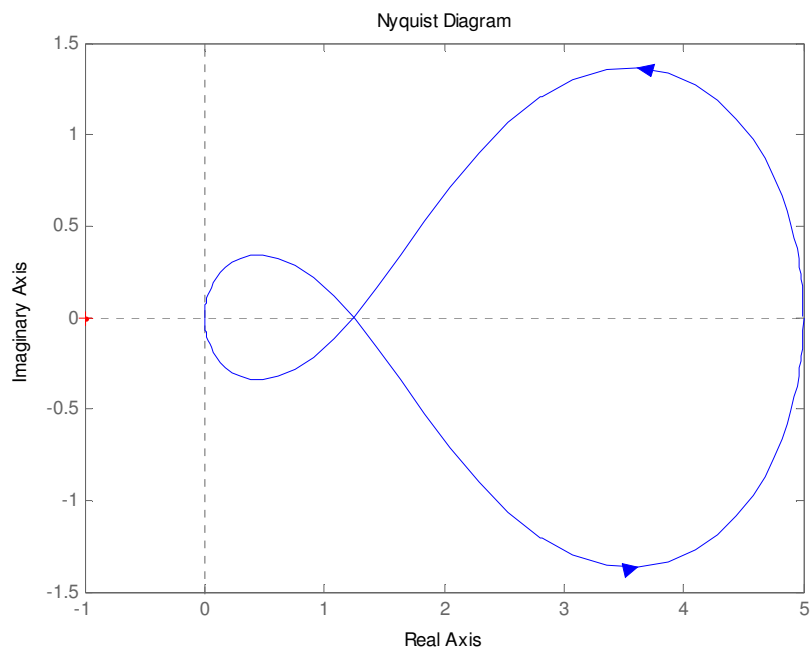


Fig. 27. Nyquist plot of the plant

Same procedure is carried out like Example IV.2 in order to obtain robust PID controller gain sets. Using root locus ideas [16], a necessary condition for the existence of stabilizing  $(K_i, K_d)$  values is that  $K_p \in (-1.8, -0.2)$ . Select  $K_p$  as  $-0.5$  in this example, then it is discovered that the stability convex set in red has been got smaller into blue area for the  $H_\infty$  constraint ( $= 1$ ) in Fig. 28. If we choose  $\gamma = 2$ , less restraint requirement, then the blue  $H_\infty$  constraint area in Fig. 28 is growing as shown in Fig. 29.

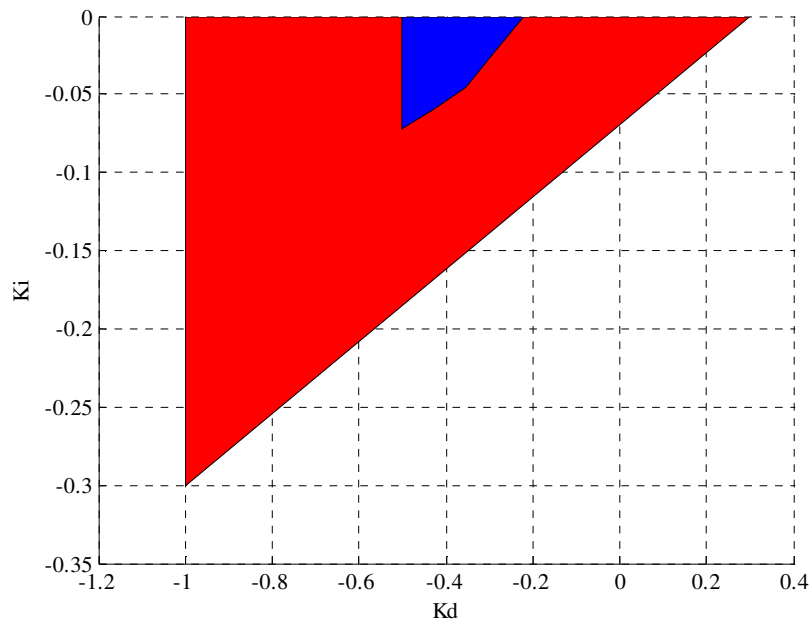


Fig. 28. Entire  $K_i, K_d$  gain for  $H_\infty$  constraint,  $\gamma = 1$

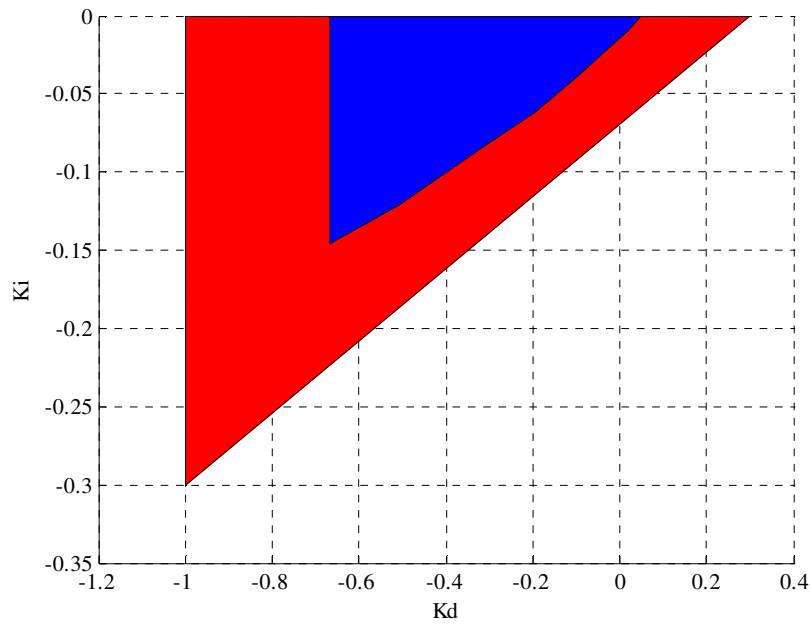


Fig. 29. Entire  $K_i, K_d$  gain for  $H_\infty$  constraint,  $\gamma = 2$

In Fig. 30 the 3D admissible gain set of  $(K_d, K_p, K_i)$  values is obtained using the above theory, by sweeping over distinct  $K_p \in (-0.55 -0.2)$  and indeed, it is confirmed to be identical to [12].

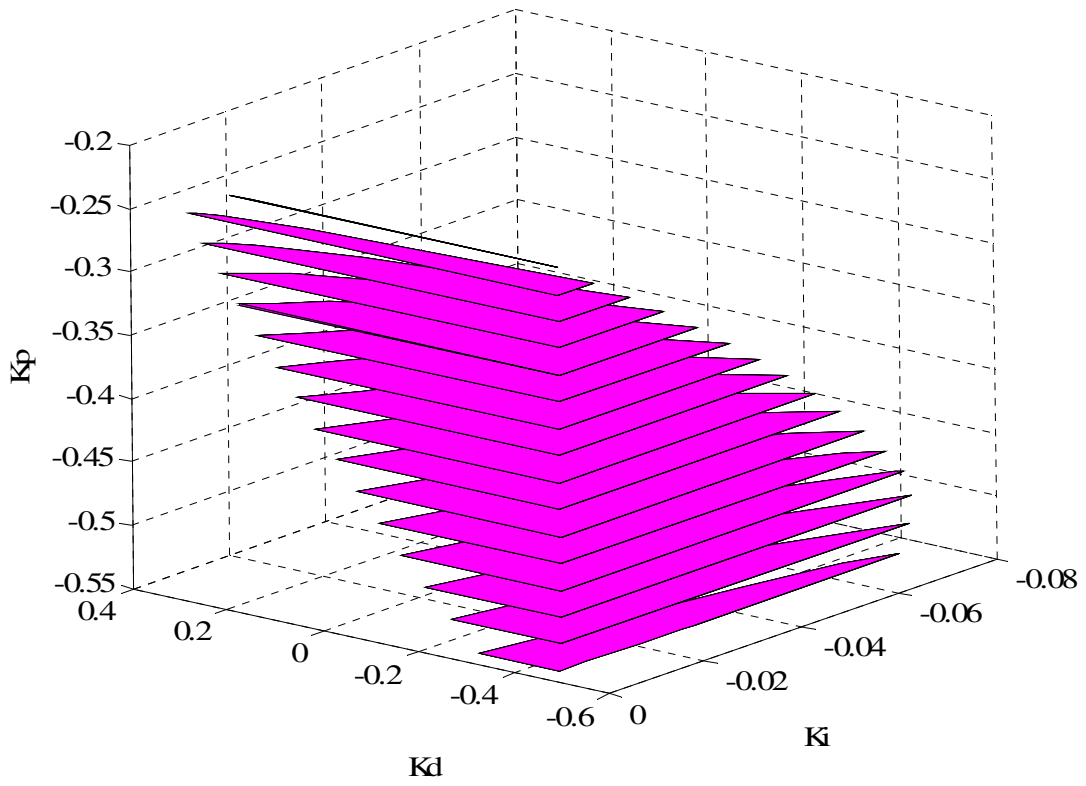


Fig. 30. Entire PID controller gain sets for  $H_\infty$  constraint,  $\gamma = 1$

## CHAPTER V

### ROBUST PID CONTROLLER SYNTHESIS FROM EMPIRICAL DATA

#### A. Introduction

Robust control which deals uncertain plants – systems with unknown dynamics and/or disturbance signals, using fixed controllers has been a significant issue for decades. Hundreds and thousands of papers handle robust control problems and numerous techniques have been proposed. Robust stability of stable feedback systems for uncertain time-invariant plants is classified in a big portion among robust control issues. It can be divided into three sections: 1. Kharitonov and polynomial approaches, 2. Lyapunov and matrix approaches and 3. Transfer function approaches [17].

First, “Kharitonov theorem” [18] provides a necessary and sufficient condition for the stability of a polynomial whose coefficients vary independently in given bounded intervals. This theorem has given motivation to make use for robust control, yet, for instance, in [19] H. Chapellat *et. al.* consider coefficient space to calculate the radius of the largest stability ball, using the characteristic polynomial. They focus on two cases: first in coefficient space with respect to perturbations in the coefficients of the characteristic polynomial, and then for a control system containing perturbed parameters in the transfer function description of the plant. Another class is Lyapunov and matrix approaches that handle robustness analysis and design for linear uncertain systems represented by state-space description. Accordingly, the uncertainty is assumed to arise

in the form of perturbations in the matrices of the state-space models, so this category is left out in this chapter. The last class is transfer function approaches: structured and unstructured perturbations that are modeled in the frequency domain. In [9] S. Mitra extends [4] to robust stability by applying interval coefficients [20], however, it requires additional computations and we want to continue using the same algorithm introduced in Chapter III and IV with holding consideration of phase margin performance.

Thus, in this chapter, we enhance Chapter III, the nominal performance – phase margin – to the robust performance stage. We try a frequency domain approach, that is, we consider the unknown bounded noise when measuring the plant's frequency response. With this structured uncertainties, we take robust linear programming [21] into account and develop a series of conditions, which is called “Cone Programming” instead of linear programming, since they are resulted in the form of non-linear inequalities. Using this programming, we are able to exploit the same algorithm in Chapter III, and the same procedure is carried out to get the entire controller gain sets satisfying robust performance criterion. The convex controller set is illustrated graphically by using Yalmip in Matlab and this result is compared to nominal performance convex sets.

#### B. Determining Robust PID Controller Set

Again, we only need to consider the series of constraints – LPs in Chapter III and IV. And the rest of literature is alike. Start with the linear programming (3.24) and (3.25) recalled here as



When  $i_k = 1$ ,

$$A_k(\omega) \begin{bmatrix} K_d \\ K_i \end{bmatrix} > b_k(\omega), \text{ for } k = 1, 2, 3, \dots, l \quad (3.24)$$

When  $i_k = -1$ ,

$$A_k(\omega) \begin{bmatrix} K_d \\ K_i \end{bmatrix} < b_k(\omega), \text{ for } k = 1, 2, 3, \dots, l \quad (3.25)$$

where  $A(\omega)$  is an  $l$  by 2 matrix and  $b(\omega)$  an  $l$  vector as shown below

$$\begin{aligned} A(\omega) &= |H_p(j\omega)|^2 \begin{bmatrix} -\omega^2 & 1 \end{bmatrix} \\ b(\omega) &= -\omega(U(\omega)H_{pr}(\omega) - V(\omega)H_{pi}(\omega)) \end{aligned} \quad (3.20)$$

and

$$\begin{aligned} H_{pr}(\omega) + jH_{pi}(\omega) &= H_p(-j\omega) \\ U(\omega) &= (\sin \theta - T\omega \cos \theta) \\ V(\omega) &= (\cos \theta + T\omega \sin \theta) \end{aligned} \quad (3.17)$$

In [21] robust linear programming is introduced as of following and it leads to Lemma

V.1 for this research:

$$\text{minimize } c^T x$$

subject to  $a_i^T x \leq b_i$  for all  $a_i \in \xi_i$ ,  $i = 1, \dots, m$ , where

$$a_i \in \xi_i = \{ \tilde{a}_i + P_i u \mid \|u\|_2 \leq 1 \} \quad (5.1)$$

The robust constraint,  $a_i^T x \leq b_i$  for all  $a_i \in \xi_i$ , can be expressed as

$$\tilde{a}_i^T x + \|P_i^T x\|_2 \leq b_i \quad (5.2)$$

because  $\sup\{ a_i^T x \mid a_i \in \xi_i \} = \tilde{a}_i^T x + \sup\{ u^T P_i^T x \mid \|u\|_2 \leq 1 \}$

$$= \tilde{a}_i^T x + \|P_i^T x\|_2 \leq b_i \quad (5.3)$$

**Lemma V.1** When  $\|\beta\|_2 \leq \delta, \|\varepsilon\|_2 \leq \psi$ ,  $\delta \in \mathfrak{R}$ ,  $\psi \in \mathfrak{R}$ ,  $\alpha \in \mathfrak{R}^n$ ,  $\beta \in \mathfrak{R}^n$ ,  $x \in \mathfrak{R}^n$ ,  $\gamma \in \mathfrak{R}$ ,  $\varepsilon \in \mathfrak{R}$ , the system of uncertain given linear inequality,

$$\alpha^T x + \beta^T x \leq \gamma + \varepsilon \quad (5.4)$$

should hold for every  $\beta$  and  $\varepsilon$ , if and only if

$$\alpha^T x + \delta \|x\|_2 \leq \gamma - \psi \quad (5.5)$$

**Proof.** The proof is very straightforward. It considers the worst case when the lesser side has the greatest value and the more side has the smallest value, such that the given condition should be always true, if and only if the worst case is satisfied. Moreover, the absolute value of inner product should be the greatest when two vectors are coinciding with each other such as  $\alpha^T x = \alpha \cdot x = |\alpha| |x| \cos \theta \leq |\alpha| |x|$ , where  $\theta$  is the angle between vector  $\alpha$  and vector  $x$ . So the given criterion becomes  $\beta^T x \leq \|\beta\|_2 \|x\|_2 \leq \delta \|x\|_2$ .  $\square$

Now, recalled linear inequalities (3.24) and (3.25) are extended to a system of uncertain linear inequalities in (5.6).

$$i_k \{A_k(\omega_k)^T K + \beta^T K\} > i_k \{b_k(\omega_k) + \varepsilon\} \quad (5.6)$$

For the robust performance satisfactory, we employ Lemma V.1 into (5.6) in a same fashion to get robust programming.

**Proposition V.1** Assume the unknown parameters should be bounded as of following;

$$\begin{aligned} \|\beta\|_2 &< \delta_k, \\ \|\varepsilon\|_2 &< \psi_k, \quad \delta_k, \psi_k \in \mathfrak{R} \end{aligned} \quad (5.7)$$

where  $A_k(\omega_k) \in \mathfrak{R}^2$ ,  $\beta \in \mathfrak{R}^2$ ,  $K \in \mathfrak{R}^2$ ,  $b_k(\omega_k) \in \mathfrak{R}$ ,  $\varepsilon \in \mathfrak{R}$ . By lemma V.1, the uncertain linear inequalities (5.6) should hold for every  $\beta$  and  $\varepsilon$ , if and only if

When  $i_k = 1$ ,

$$A_k(\omega_k)K^T - \delta_k \|K\|_2 > b_k(\omega_k) + \psi_k, \text{ for } k = 1, 2, 3, \dots, l$$

When  $i_k = -1$ ,

$$A_k(\omega_k)K^T + \delta_k \|K\|_2 < b_k(\omega_k) - \psi_k, \text{ for } k = 1, 2, 3, \dots, l \quad (5.8)$$

And then, the solution set  $K$  by (5.7) and/or (5.8) satisfies (5.6) for every  $\beta$  and  $\varepsilon$ .  $\square$

Seeing (5.7), the need arises that we have information of upper and lower bound  $\delta$  and  $\psi$  to solve robust programming (5.8). Even if a lot of strategies clarifying the bound limits of uncertainties can be demised to approach to the exact answer, we assume simply the estimation aberration lies within 10% like Figs. 31 and 32. Let  $|\hat{H}_p(j\omega_o)|$  be the exact plant's frequency data and  $|H_p(j\omega_o)|$  be the measured value of the plant, then

$$|\hat{H}_p(j\omega_o) - H_p(j\omega_o)| < 0.1 |H_p(j\omega_o)| \quad (5.9)$$

$$|H_p(j\omega_o)| = \alpha |\hat{H}_p(j\omega_o)|, 0.9 \leq \alpha \leq 1.1 \quad (5.10)$$

$$|H_p(j\omega_o)|^2 = \alpha^2 |\hat{H}_p(j\omega_o)|^2, 0.81 \leq \alpha^2 \leq 1.21 \quad (5.11)$$

where  $\omega_o$  is specified frequency. Because  $A_k(\omega_o)$  is related with  $|H_p(j\omega_o)|^2$  and  $b_k(\omega_o)$  is also with  $|H_p(j\omega_o)|$  as defined in (3.20), it is very reasonable that we set

$$\begin{aligned} \delta_k &= 0.2 \|A_k(\omega)\|_2 \\ \psi_k &= 0.1 \|b_k\|_2 \end{aligned} \quad (5.12)$$

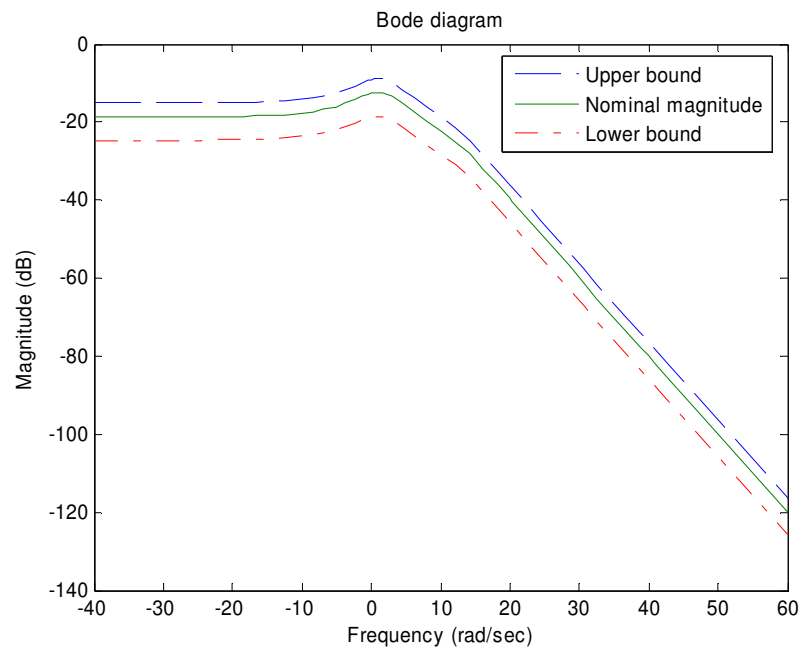


Fig. 31. Bode diagram with upper bound and lower bound of uncertainties

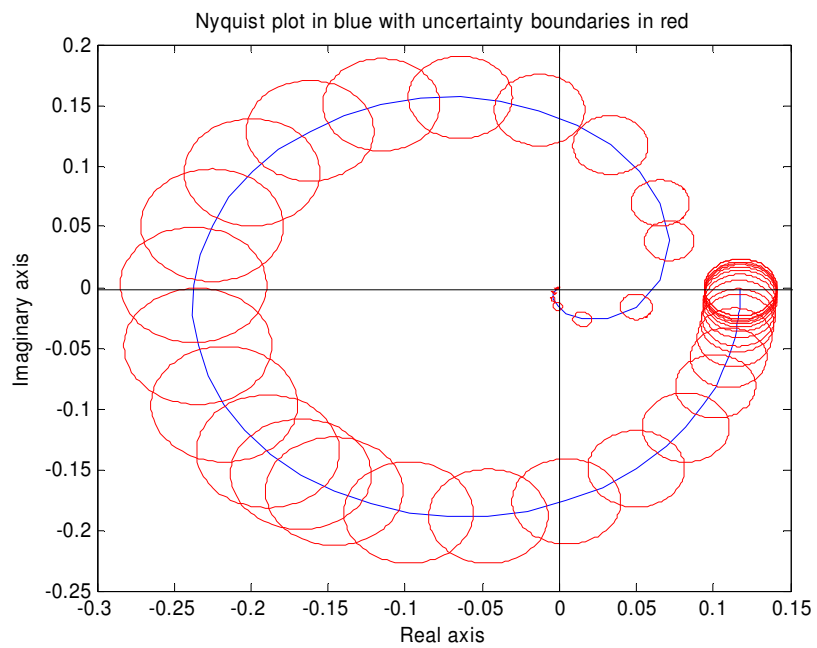


Fig. 32. Nyquist plot with uncertainties' boundaries

**Proposition V.2** From proposition V.1 and by the presumed error scope (5.12), the equations (5.8) are expressed in a different way of look by

When  $i_k = 1$ ,

$$A_k(\omega)K^T - 0.2\|A_k(\omega)\|_2\|K^T\|_2 > b_k + 0.1|b_k|, \text{ for } k = 1, 2, 3, \dots, l \quad (5.12)$$

When  $i_k = -1$ ,

$$A_k(\omega)K^T + 0.2\|A_k(\omega)\|_2\|K^T\|_2 < b_k - 0.1|b_k|, \text{ for } k = 1, 2, 3, \dots, l \quad (5.12)$$

where  $K = [K_d \quad K_i]^T$ . □

(5.12) and (5.13) construct non-linear inequalities for the convex set of robust performance PID controller gains. It is noted that they are switched to be used for this robust performance instead of LPs in (3.24) and (3.25) but the rest of systematic calculation way is remained as identical. Consider the examples in the following section.

### C. Examples

**Example V.1.** Consider the given plant's frequency response shown in Figs. 33 and 34. Find nominal stability, nominal performance and robust performance for the minimum phase margin =  $30^\circ$ . Assume the estimation error is bounded within 10%.

By similar calculation to (3.26), we obtain plant's order difference,  $n - m = 5$  and the non-minimum phase zero,  $u = 2$ . By Theorem III.1, the required signature condition is determined as

$$\sigma(\delta(s, K)) = \left( \text{sgn} \left[ \frac{d\delta_i(\omega)}{d\omega} \right]_{\omega=\omega_1} \left\{ i_1 - 2i_2 + 2i_3 \cdots + 2(-1)^{l-1}i_{l-1} + (-1)^l i_l \right\} \frac{1}{2} + 1 \right) = 11 \quad (5.14)$$

where  $i_k (k = 1, 2, 3, \dots, l)$  is the root of  $\delta_i(\omega)$ .

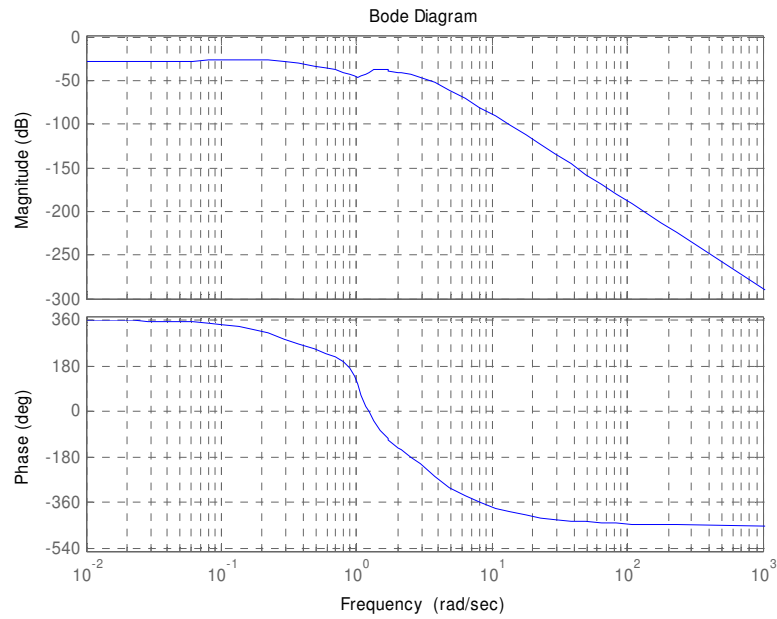


Fig. 33. Bode diagram of the plant

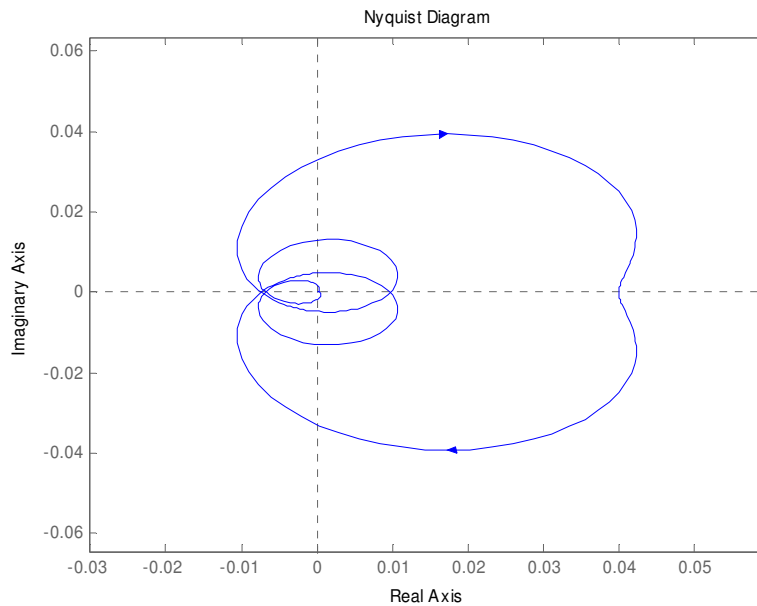


Fig. 34. Nyquist diagram of the plant

It is obvious that at least 11 roots in the imaginary part of  $\delta(j\omega)$  are required to yield feasible controller gains. By (3.29), the admissible  $K_p$  range is determined as  $[-22.352, 116.85]$  as shown in Fig. 35. Select  $K_p = 70$ , then the real roots of  $\delta_i(\omega)$  are shown as of followings:

$$\begin{aligned} \omega = & -24.694, -3.1565, -1.7535, -0.95446, -0.65391, 0 \\ & 0.78367, 1.0532, 2.1965, 4.7585, 5803.4 \text{ (rad/sec)} \end{aligned} \quad (5.15)$$

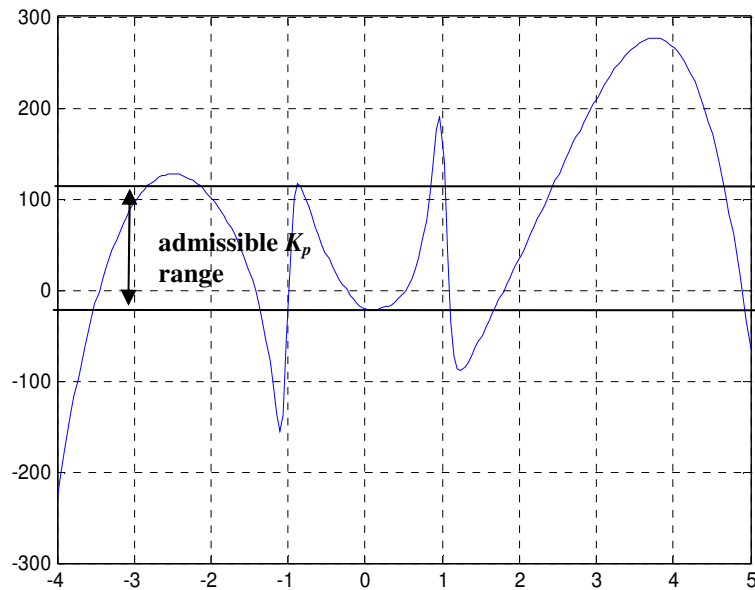


Fig. 35.  $f(\omega)$  for illustrating admissible  $K_p$  range

(5.14) is specified by the obtained roots and sign value of derivative of  $\delta_i(\omega)$  at  $\omega_1 = -1$ .

Now we get the signature condition from (5.14)

$$-1(i_1 - 2i_2 + 2i_3 - 2i_4 + 2i_5 - 2i_6 + 2i_7 - 2i_8 + 2i_9 - 2i_{10} + i_{11}) = 20 \quad (5.16)$$

(5.15) leads only one feasible set  $F^*$  of

$$F^* = \{ i_1, i_2, i_3, i_4, i_5, i_6, i_7, i_8, i_9, i_{10}, i_{11} \} = \{ -1, 1, -1, 1, -1, 1, -1, 1, -1, 1, -1 \} \quad (5.17)$$

Finally we can construct cone programming by (5.12) and (5.13) as shown below:

$$\begin{aligned}
-1.1e-005 K_d \quad +1.8e-008 K_i \quad + 2.2e-006 \sqrt{K_d^2 + K_i^2} &< 1.1 - 0.1 \\
-17.552 K_d \quad +1.7616 K_i \quad - 3.528 \sqrt{K_d^2 + K_i^2} &> -1266.4 + 126.64 \\
-41.323 K_d \quad +13.439 K_i \quad + 8.6907 \sqrt{K_d^2 + K_i^2} &< 1187.9 - 118.79 \\
-2.4637 K_d \quad +2.7044 K_i \quad - 0.73167 \sqrt{K_d^2 + K_i^2} &> -462.3 + 46.23 \\
-8.3736 K_d \quad +19.583 K_i \quad +4.2596 \sqrt{K_d^2 + K_i^2} &< 184.03 - 18.403 \\
\quad \quad \quad 160 K_i \quad -32 \sqrt{K_d^2 + K_i^2} &> 0 \\
-5.5753 K_d \quad +9.0782 K_i \quad +2.1307 \sqrt{K_d^2 + K_i^2} &< 556.35 - 55.635 \\
-2.74 K_d \quad +2.4703 K_i \quad -0.73783 \sqrt{K_d^2 + K_i^2} &> -490.75 + 49.075 \\
-34.484 K_d \quad +7.1476 K_i \quad +7.0434 \sqrt{K_d^2 + K_i^2} &< 1496.9 - 149.69 \\
-2.4614 \quad +0.10871 K_i \quad -0.49277 \sqrt{K_d^2 + K_i^2} &> -494.81 + 49.481 \\
-1.2e-024 \quad +3.7e-032 K_i \quad + 2.5e-025 \sqrt{K_d^2 + K_i^2} &< 3.7e-010 \quad (5.18)
\end{aligned}$$

The outcome of the cone programming (5.18) for this example is illustrated in Fig. 36. It is observed that robust performance gain set in black dot area becomes more conservative than nominal performance gain range in sky blue. Note that the yellow zone – nominal stability - envelope both nominal and robust range, however, it is not always of the same happening as mentioned in Example III.2.

At the red point,  $K_d = 50$  and  $K_i = 16.25$ , the compensator is verified by the margin of open loop system and step response of closed feedback system comparing



with uncompensated one as shown in Figs. 37 and 38. Now we can confirm the obtained gain set has reasonable frequency and time response performance. The uncompensated system can not follow the reference step input, on the other hand, the compensated system contents required minimum phase margin, which is  $30^\circ$  and also it is stabilized to the step input with no error at steady state in fairly good time.

The other points in robust performance region work well similarly to those of tested point, thus even if there exists estimation inaccuracy, one can have a great number of alternatives to choose the controller for any objective.

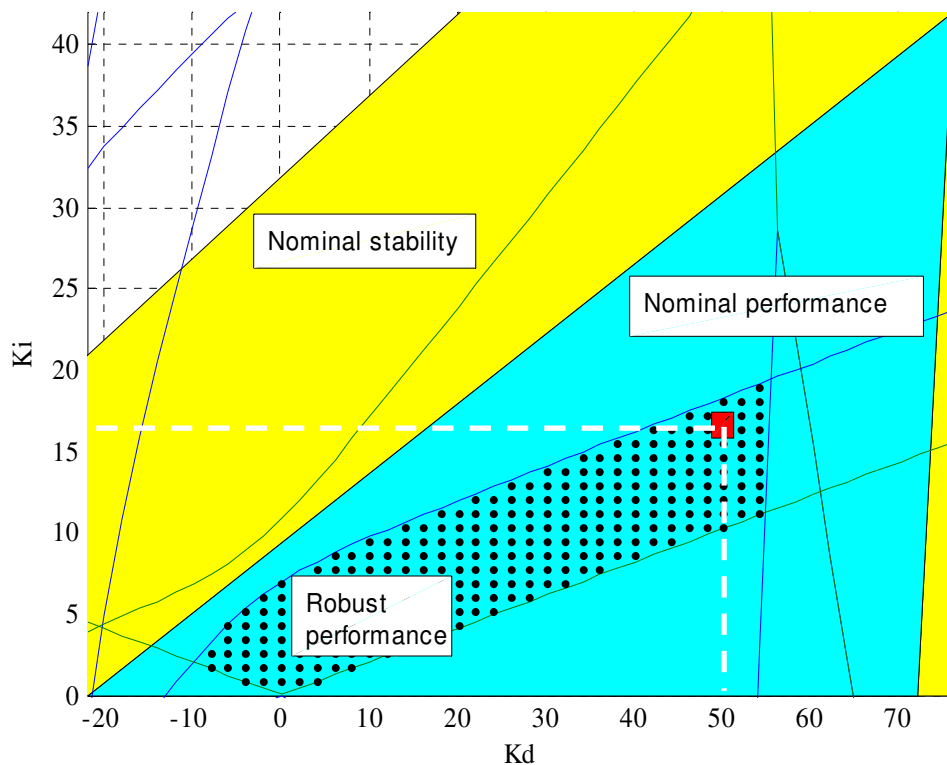


Fig. 36. Entire robust performance PID gain set for  $K_p = 70$

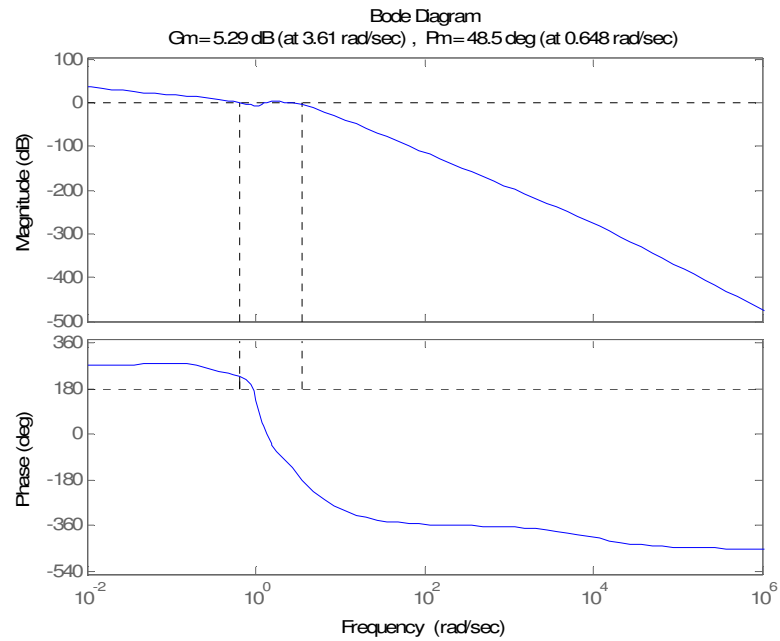


Fig. 37. Bode diagram of compensated sys. with  $K_d = 50$ ,  $K_p = 70$  and  $K_i = 16.25$

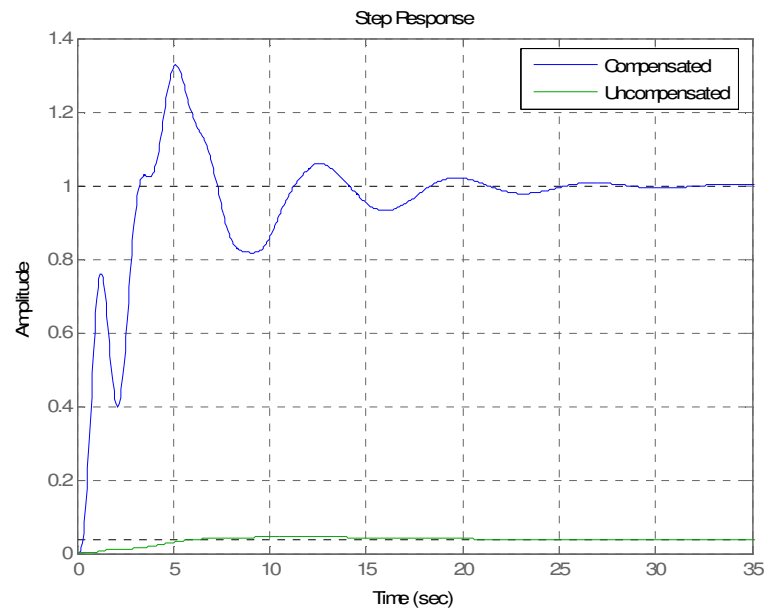


Fig. 38. Comparison of each step response

**Example V.2.** The same plant shown in example III.1 is treated for the robust performance to be achieved when it is considered that the estimation of the plant can not be precise. The comparison between nominal performance and robust performance is commented and shown by the graph. From Example III.1,  $K_p = 3$ , the roots of  $\delta_i(\omega)$  have been given by

$$\omega_k = (-17348, -6.1137, -1.3051, -0.6905, 0, 1.1206, 2.0628, 11.839) \quad (5.19)$$

$A(\omega)$  and  $B(\omega)$  have been obtained already earlier as

$$10^2 A(\omega) = \begin{bmatrix} -3.3227e-007 & 1.104e-015 \\ -2.9408 & 0.078678 \\ -8.8664 & 5.2056 \\ -1.5719 & 3.2968 \\ 0 & 1.3841 \\ -7.2052 & 5.738 \\ -7.4487 & 1.7505 \\ -0.77056 & 0.0054975 \end{bmatrix}, \quad 10^2 B(\omega) = \begin{bmatrix} -0.011542 \\ 17.088 \\ -21.708 \\ 10.514 \\ 0 \\ 18.666 \\ -25.05 \\ 8.776 \end{bmatrix} \quad (5.20)$$

thus,

$$10^3 \delta(\omega) = \begin{bmatrix} 6.6454e-007 \\ 5.8837 \\ 20.563 \\ 7.3048 \\ 2.7682 \\ 18.422 \\ 15.303 \\ 1.5412 \end{bmatrix}, \quad 10^3 \psi(\omega) = \begin{bmatrix} 0.011542 \\ 17.088 \\ 21.708 \\ 10.514 \\ 0 \\ 18.666 \\ 25.05 \\ 8.776 \end{bmatrix} \quad (5.21)$$

A series of nonlinear inequalities (Cone Programming) can be given by

$$\begin{aligned}
-3.3227 \cdot 10^{-7} K_d + 1.104 \cdot 10^{-15} K_i - 6.6454 \cdot 10^{-8} \cdot \sqrt{K_d^2 + K_i^2} &> -0.011542 + 0.0011542 \\
-2.9408 K_d + 0.078678 K_i + 0.58837 \cdot \sqrt{K_d^2 + K_i^2} &< 17.088 - 1.7088 \\
-8.8664 K_d + 5.2056 K_i - 2.0563 \cdot \sqrt{K_d^2 + K_i^2} &> -21.708 + 2.1708 \\
-1.5719 K_d + 3.2968 K_i + 0.73048 \cdot \sqrt{K_d^2 + K_i^2} &< 10.514 - 1.0514 \\
1.3841 K_i - 0.27682 \cdot \sqrt{K_d^2 + K_i^2} &> 0 \\
-7.2052 K_d + 5.738 K_i + 1.8422 \cdot \sqrt{K_d^2 + K_i^2} &< 18.666 - 1.8666 \\
-7.4487 K_d + 1.7505 K_i - 1.5303 \cdot \sqrt{K_d^2 + K_i^2} &> -25.05 + 2.505 \\
-0.77056 K_d + 0.0054975 K_i + 0.15412 \cdot \sqrt{K_d^2 + K_i^2} &< 8.776 - 0.8776 \quad (5.22)
\end{aligned}$$

The result of (5.22) can be shown in Fig. 39 in the same manner of Example V.1. The entire  $K_d, K_i$  set region of  $K_p = 3$  for robust performance is displayed in red and nominal performance with stability is in blue and nominal stabilizing set is given in yellow.

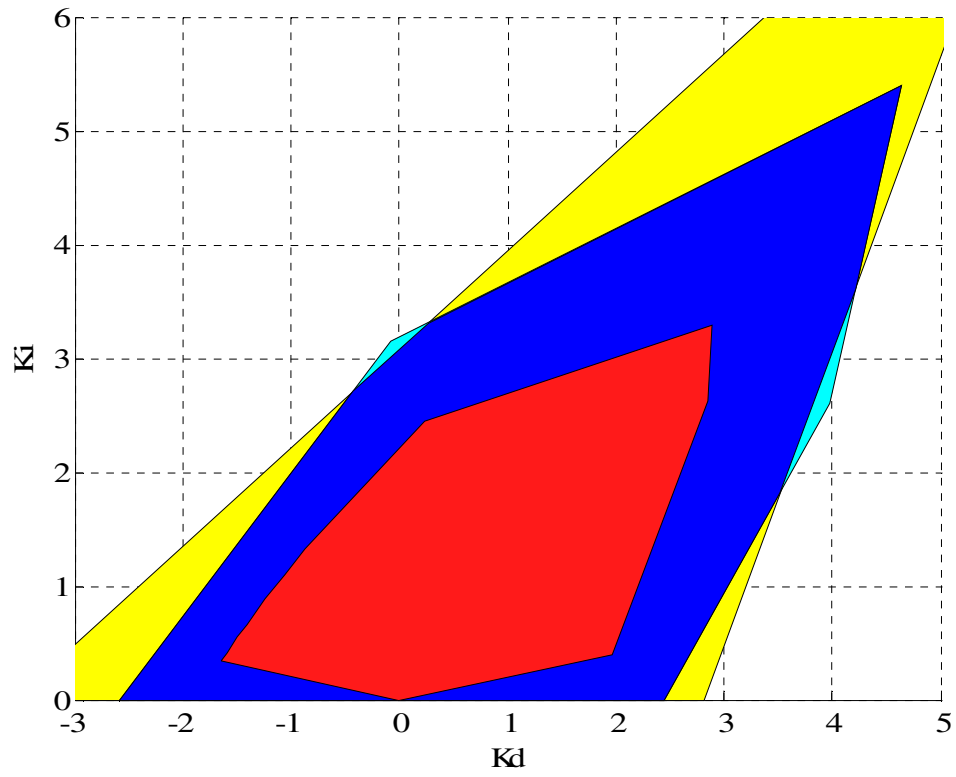


Fig. 39. Entire robust performance PID gain set for  $K_p = 3$

## CHAPTER VI

### CONCLUSION AND FUTURE WORK

#### A. Summary

In the previous chapters the open problem of the PID controller synthesis has been taken into consideration. The main objective is to procure the entire controller gain sets of PID such as  $[K_d K_p K_i]^T$  satisfying the given performance specification. The achievement can be appreciated as an advanced step bearing in mind that this thesis deals with complex rational function case, which is more general than real case. In order to drive the research into the end, the mathematical background for the complex case is presented, modified and developed for the objective of this thesis. The Hermite-Biehler theorem for real Hurwitz polynomial is extended to a complex non-Hurwitz polynomial and its characteristics are proposed, analyzed and arranged for being taken to systematic computational approach, which is called a noble feature of this thesis algorithm. Besides, automatic sign assignment logic is developed for the methodical computation that is also an important objective of this thesis. The algorithm and basic idea for contending phase margin property is introduced. By this computation, the controller gains can be easily selected not knowing the plant itself. Furthermore, in case that the controller with specific gains does not work, the user can effortlessly take alternative from graphical user interface of the entire gain sets. Similarly,  $H_\infty$  constraint specification can be obtained with the phase margin performance case. The results are shown as more

conservative gain sets graphically as well. It can be said very fairly that one may not be able to estimate plant's exact frequency data. Thus, the robust performance property is studied so as to obtain much more absolutely stable and reliable system. Not to mention, the robust performance is also intended for the systematic calculation by a computer and implemented graphically. It is concluded that it depends on the plant's frequency magnitude, because from its assumption when the estimation value is large, the noise value can be amplified.

#### B. Future Work

In electrical engineering, discrete time cases are studied in depth for various aspects [9]. This thesis' algorithm can be applied to discrete time system and one can exploit this to enhance the Graphic User Interface (GUI) in [9]. This thesis only considered Single Input Single Output system (SISO system). In [5] Multi Input Single Output and Single Input Multi Output systems have been handled, however, it is needed to extend this research to Multi Input Multi Output system. In some reason, the fixed structured higher order controller arise the needs that we can approach in a similar way with this thesis. Even though the robust performance is shown in the later part of this thesis, various kinds of the developed robustness should be obtained such as an absolute stability problem. It is evident there exists a lot mathematical theorems and propositions which we can take advantage of for the Control System field.

## REFERENCES

- [1] K. Ogata, *Modern Control Engineering*, Upper Saddle River, NJ: Prentice Hall, 2002.
- [2] G. J. Silva, A. Datta and S. P. Bhattacharyya, *PID Controllers for Time-Delay Systems*, Boston: Birkhäuser, 2005.
- [3] J. G. Ziegler and N. B. Nichols, "Optimum settings for automatic controllers," *Transactions of the American Society of Mechanical Engineers*, vol. 64, pp. 759-768, 1942.
- [4] L. H. Keel and S. P. Bhattacharyya, "PID controller synthesis: Free of analytical models," in *16<sup>th</sup> IFC World Congress*, Prague, Czech Republic, July 2005.
- [5] W. A. Malik, "A new computational approach to the synthesis of fixed ordered controllers," Ph.D. Dissertation, Texas A&M University, College Station, 2007.
- [6] L. H. Keel and S. P. Bhattacharyya, "A generalization of Mikhailov's criterion with applications," in *Proceedings of the American Control Conference*, Chicago, IL, vol. 6, pp. 4311-4315, June 2000.
- [7] G. F. Franklin, J. D. Powell and A. Emami-Naeini, *Feedback Control of Dynamic Systems*, Singapore: Pearson Education, 2005.



- [8] B. Narasimhan, "An automated virtual tool to compute the entire set of proportional integral derivative controllers for a continuous linear time invariant system," M.S. thesis, Texas A&M University, College Station, 2007.
- [9] S. Mitra, "Computer aided synthesis and design of PID controllers," M.S. thesis, Texas A&M University, College Station, 2007.
- [10] J. C. Doyle and K. Glover, "State-space solutions to standard  $H_2$  and  $H_\infty$  control problems," *IEEE Transactions on Automatic Control*, vol. 34, no. 8, pp. 831-847, August 1989.
- [11] S. Skogestad and I. Postlethwaite, *Multivariable Feedback Control*, West Sussex, England: Wiley, 2001.
- [12] M. T. Ho, "Synthesis of  $H_\infty$  PID controller: A parametric approach," *Automatica* vol. 39, pp 1069-1075, 2003.
- [13] R. N. Tantar, L. H. Keel and S. P. Bhattacharyya, " $H_\infty$  design with first-order controllers," *IEEE Transactions on Automatic Control*, vol. 51, no. 8, pp. 1343-1347, August 2006.
- [14] S. P. Bhattacharyya, H. Chapellat and L. H. Keel, *Robust Control: The Parametric Approach*, Upper Saddle River, NJ: Prentice-Hall, 1995.

- [15] J. C. Doyle, B. A. Francis and A. R. Tannenbaum, *Feedback Control Theory*, New York: Macmillan Publishing Company, 1992.
- [16] M. T. Ho, A. Datta and S. P. Bhattacharyya, "Generalizations of the Hermite-Biehler Theorem: The Complex Case", *Linear Algebra and Its Applications*, vol. 320, no. 1-3, pp. 23-36, 2000.
- [17] P. Dorato and R. K. Yedavalli, *Robust Control*, New York: IEEE Press, 1990.
- [18] V. L. Kharitonov, "Asymptotic stability of an equilibrium position of systems of linear differential equations," *Differential 'nye Uraveniya*, vol. 14, pp. 2086-2088, 1978.
- [19] H. Chapellat, S. P. Bhattacharyya and L. H. Keel, "Stability margins for Hurwitz polynomials," in *Proceedings of the 27<sup>th</sup> IEEE Conference on Decision and Control*, vol. 2, pp. 1392-1398, December 1988.
- [20] L. Jaulin, M. Kieffer, O. Didrit and E. Walter, *Applied Interval Analysis, with Examples in Parameter and State Estimation, Robust Control and Robotics*, London: Springer, 2001.
- [21] S. Boyd and L. Vandenberghe, *Convex Optimization*, Cambridge, United Kingdom: Cambridge University Press, 2006.

## VITA

Name: Dongwon Lim

Address: Texas A&M University  
Department of Mechanical Engineering  
3123 TAMU College Station TX 77843-3123, USA

Education: Master of Science  
Mechanical Engineering, May 2008  
Texas A&M University, College Station, Texas, USA  
Bachelor of Science  
Mechanical Engineering, Feb 2003  
Hanyang University, Seoul, Korea

Experience: KIST (Korea Institute of Science and Technology), Seoul, Korea  
(Mar. 2005 - Aug. 2005)  
Conducted research in collaborative web frameworks  
OTIS Elevator, Seoul, Korea  
(Dec. 2002 – Mar. 2005)  
Worked as a sales representative  
HYUNDAI Heavy Industries (Summer Internship), Ulsan, Korea  
(July 2002)  
Summer internship at the Shipping Division Design center  
Military Service, Yeoncheon, Korea  
(Aug. 1998 – Oct. 2000)  
Worked in the personnel department at the division level